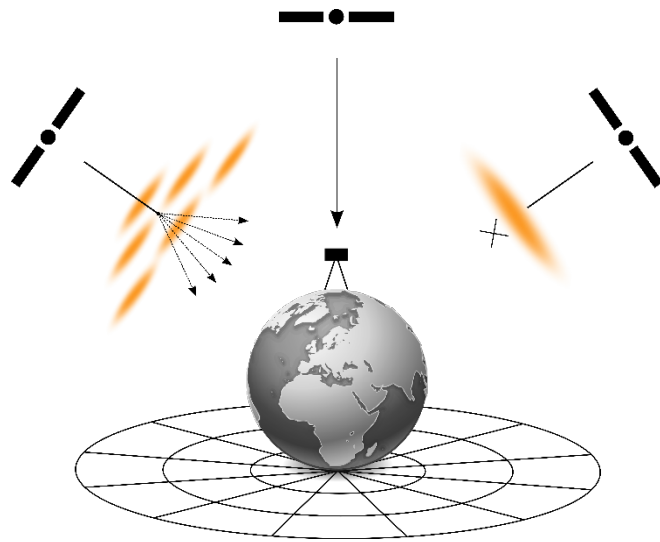


# Ingestion of Ionospheric Scintillation Skymaps into GNSS Algorithms



Matthieu Lonchay

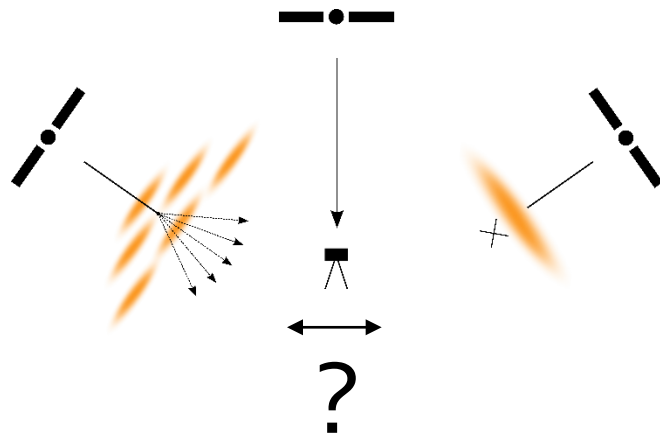
PhD Defense

ULiège

Friday 24 May 2019



# Ingestion of Ionospheric Scintillation Skymaps into GNSS Algorithms



Matthieu Lonchay

PhD Defense

ULiège

Friday 24 May 2019

## Analysis

GNSS Algorithms and Ionosphere

## Geostatistics

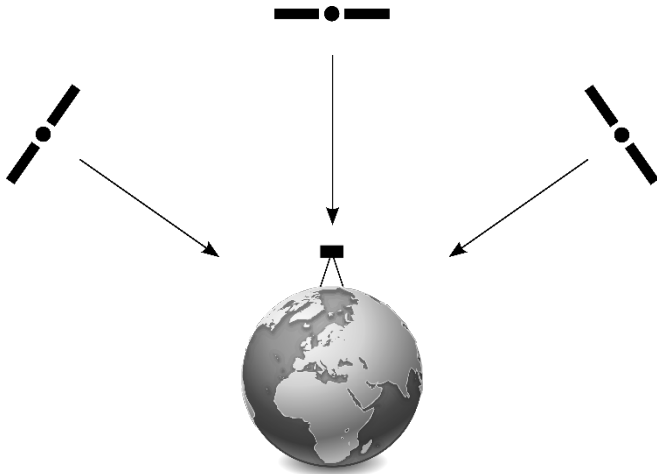
Ionospheric Scintillation Skymaps

## Prototypes

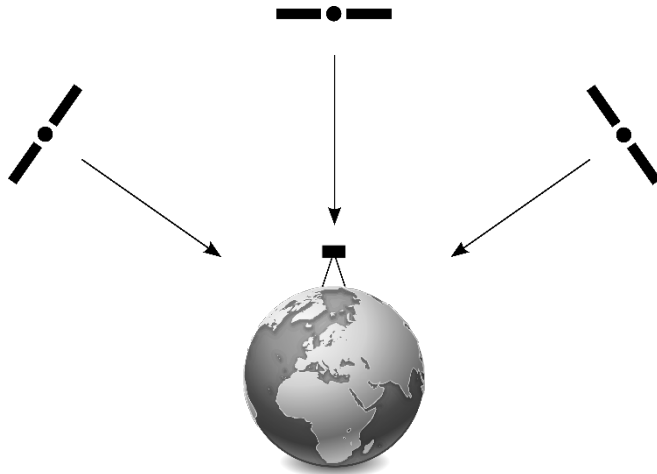
Mitigation Strategies

GNSS positioning is based on the principle of **multilateration** between a **GNSS receiver** and several **GNSS satellites** orbiting the Earth

GNSS positioning is based on the principle of multilateration

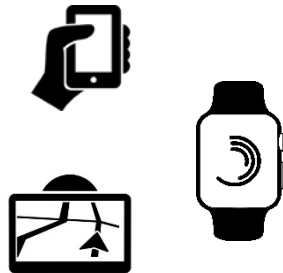


GNSS algorithms exploit code pseudorange and carrier phase measurements performed on several frequencies in order to estimate the instantaneous navigation solution of the receiver



GNSS algorithms exploit code pseudorange and carrier phase measurements related to several frequencies

GNSS algorithms exploit code pseudorange and carrier phase measurements performed on several frequencies in order to estimate the instantaneous navigation solution of the receiver

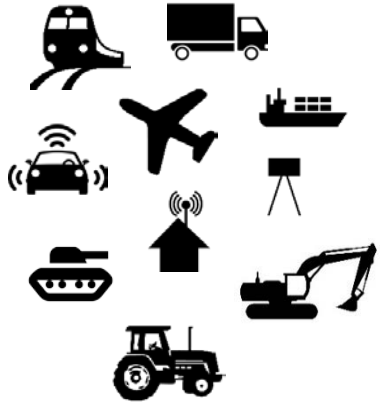


**GNSS algorithms exploit code pseudorange and carrier phase measurements related to several frequencies**

The Standard Point Positioning (SPP) algorithm is based on single-frequency code pseudorange measurements

- Light implementation
- Least-squares adjustment
- Precision of 5 m-10 m

**GNSS algorithms** exploit **code pseudorange** and **carrier phase measurements** performed on several frequencies in order to estimate the instantaneous **navigation solution** of the receiver



### **GNSS algorithms exploit code pseudorange and carrier phase measurements related to several frequencies**

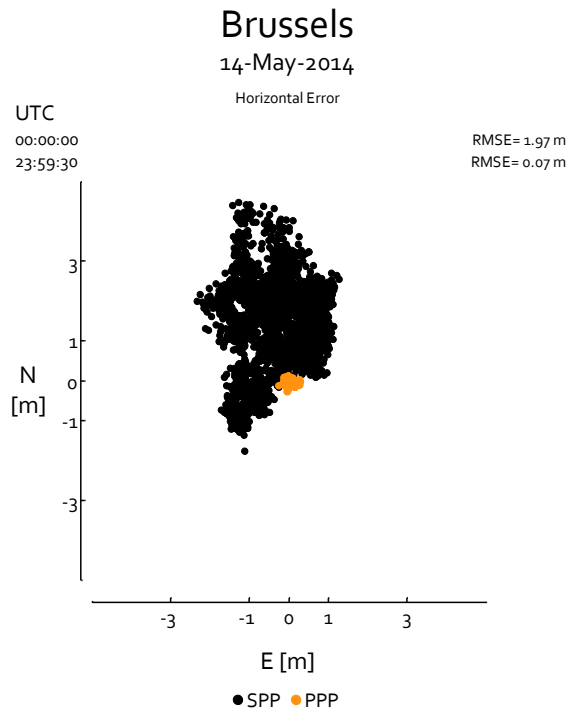
The Standard Point Positioning (SPP) algorithm is based on single-frequency code pseudorange measurements

The Precise Point Positioning (PPP) algorithm is based on dual-frequency code pseudorange and carrier phase measurements combined with regional and global corrections

- Complex implementation
- Corrections required from a provider
- Kalman filter
- **Initial integer ambiguities to estimate**
- **Centimetre-decimetre precision level**



**GNSS algorithms** exploit **code pseudorange** and **carrier phase measurements** performed on several frequencies in order to estimate the instantaneous **navigation solution** of the receiver

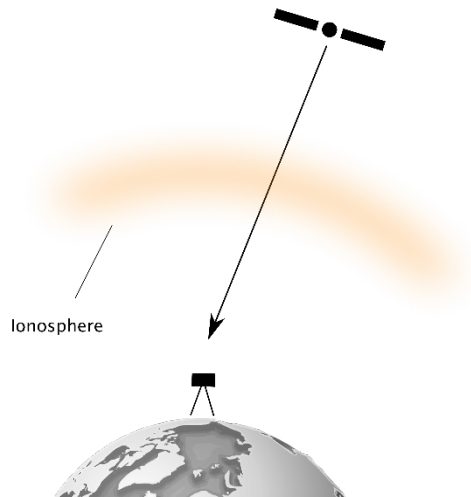


### **GNSS algorithms exploit code pseudorange and carrier phase measurements related to several frequencies**

The Standard Point Positioning (SPP) algorithm is based on single-frequency code pseudorange measurements

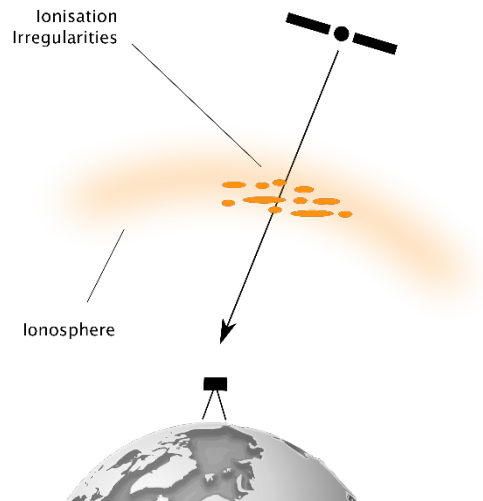
The **Precise Point Positioning (PPP)** algorithm is based on dual-frequency code pseudorange and carrier phase measurements combined with regional and global corrections

The **ionosphere** is the part of the upper atmosphere of the Earth where sufficient **ionisation** can exist to affect the **propagation of radio waves**



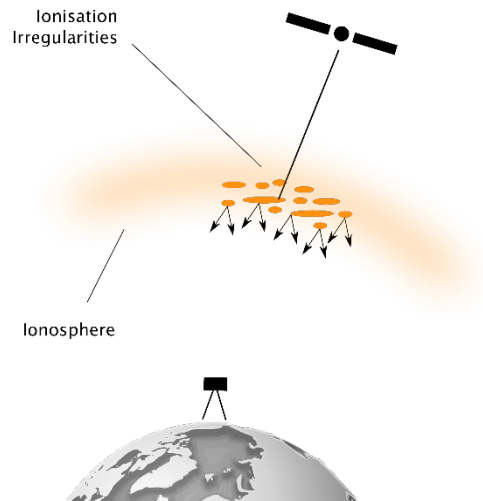
The **ionosphere** is responsible for **refraction** effects on GNSS signals which result in **delays** to be considered in the mathematical model of GNSS algorithms

The **ionosphere** is the part of the upper atmosphere of the Earth where sufficient **ionisation** can exist to affect the **propagation of radio waves**



The **ionosphere** is responsible for **refraction** effects on GNSS signals which result in **delays** to be considered in the mathematical model of GNSS algorithms

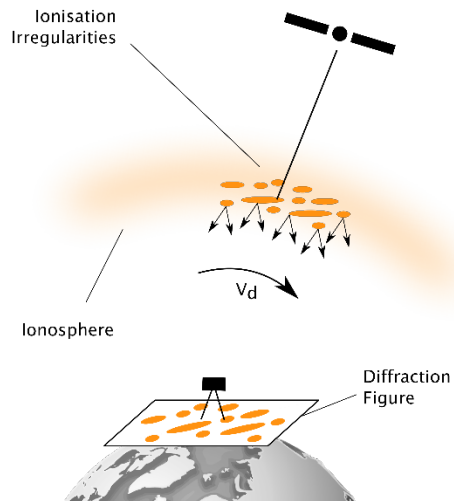
The **ionosphere** is the part of the upper atmosphere of the Earth where sufficient **ionisation** can exist to affect the **propagation of radio waves**



The **ionosphere** is responsible for **refraction** effects on GNSS signals which result in **delays** to be considered in the mathematical model of GNSS algorithms

**Small-scale irregularities** in the ionospheric free-electron density involve **diffraction** and **scattering** effects of GNSS signals

Small-scale irregularities in the ionospheric free-electron density cause diffraction and scattering effects on GNSS signals leading to rapid fluctuations of the amplitude and phase of the signals

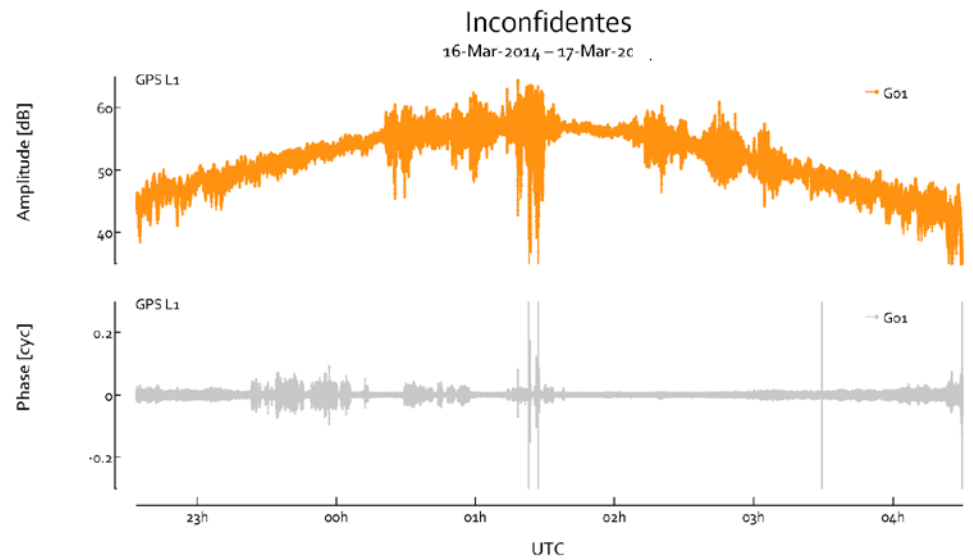
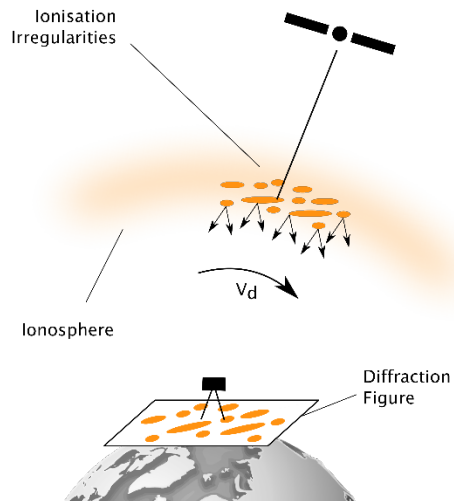


The ionosphere is responsible for refraction effects on GNSS signals which result in delays to be considered in the mathematical model of GNSS algorithms

Small-scale irregularities in the ionospheric free-electron density involve diffraction and scattering effects of GNSS signals

Scattered signals reach the receiver via multiple paths resulting in a diffraction pattern with destructive and constructive interferences of the scattered signals

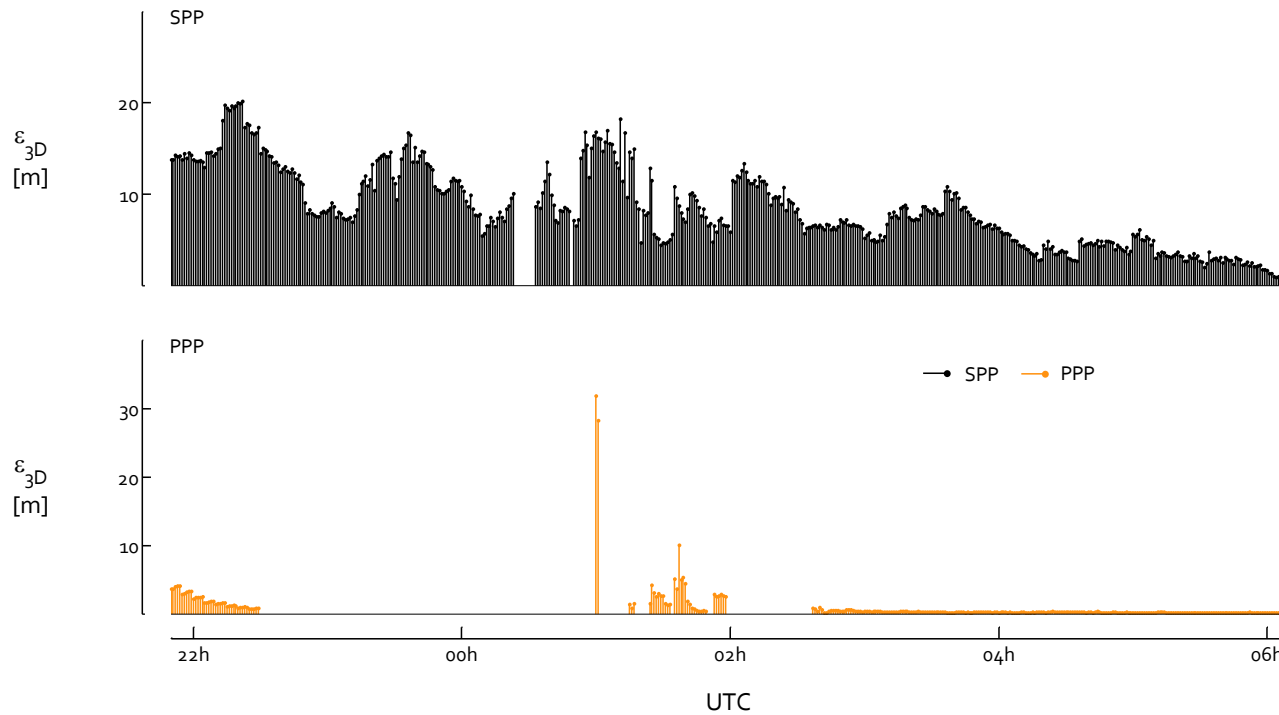
Intense ionospheric scintillations of GNSS signals severely threaten GNSS positioning performances and can make GNSSs totally inoperable



Intense ionospheric scintillations of GNSS signals severely threaten GNSS positioning performances and can make GNSSs totally inoperable

### Inconfidentes

17-Mar-2014 – 18-Mar-2014



## Analysis

GNSS Algorithms and Ionosphere

## Geostatistics

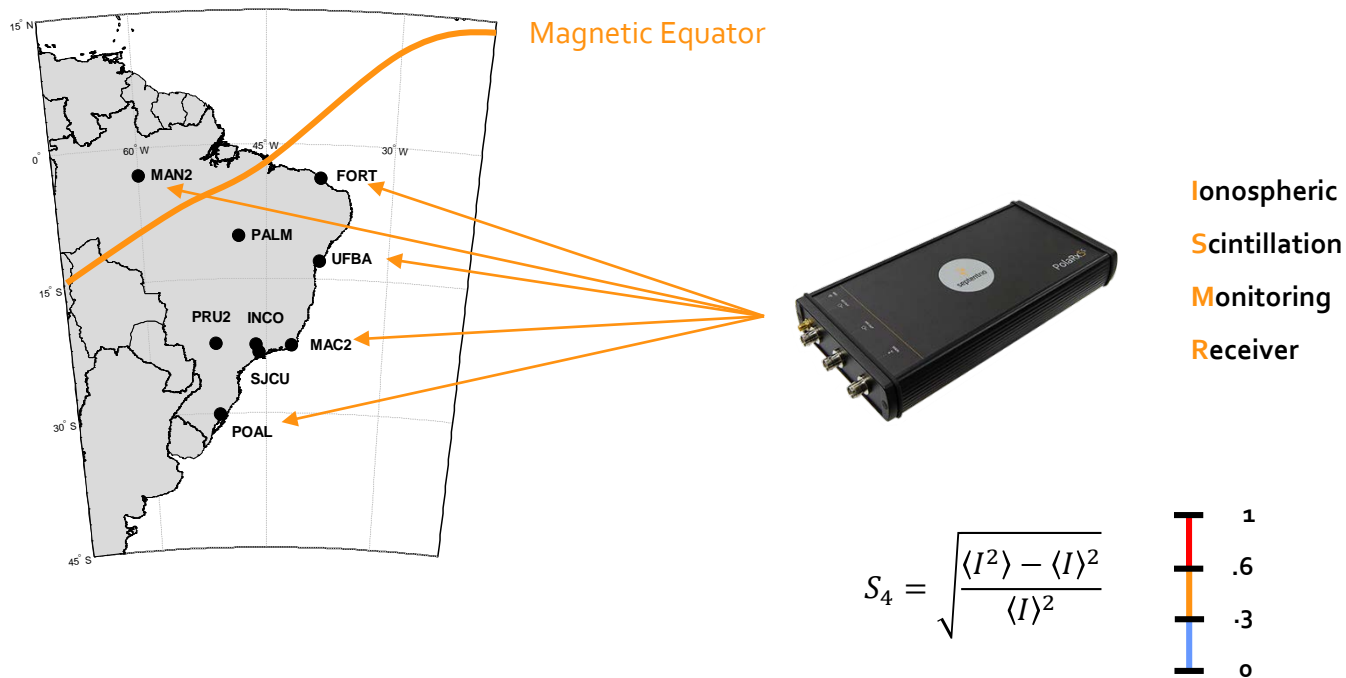
Ionospheric Scintillation Skymaps

## Prototypes

Mitigation Strategies

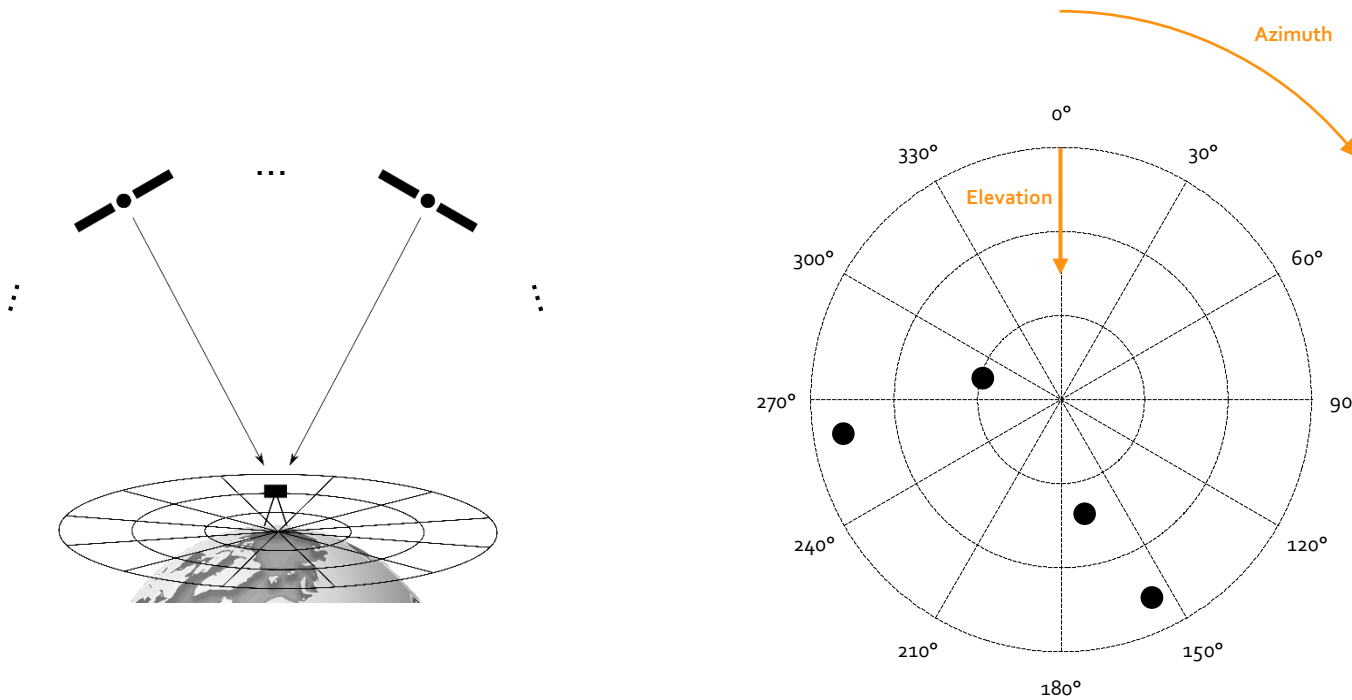


A network of **Ionospheric Scintillation Monitoring Receivers** (ISMRs) located in Brazil is exploited to generate high-density **ionospheric scintillation skyplots**



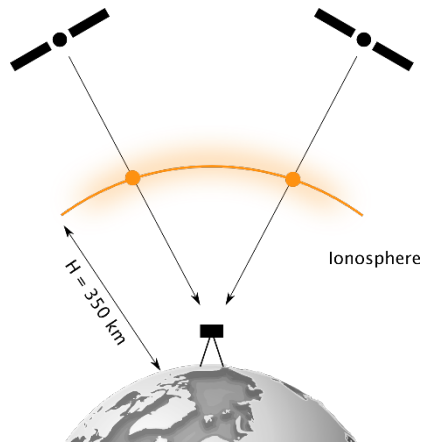
Each **station** of the network is equipped with an **ISMR** to monitor low-latitude ionospheric **scintillations**

A network of **Ionospheric Scintillation Monitoring Receivers (ISMRs)** located in Brazil is exploited to generate high-density **ionospheric scintillation skyplots**



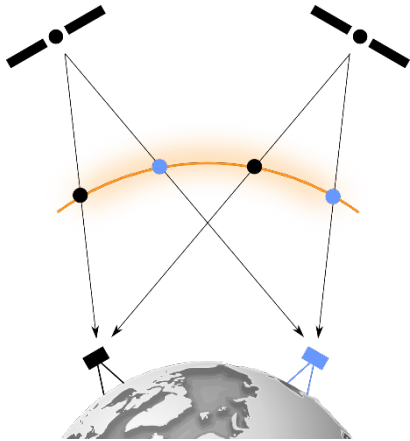
A **skyplot** is a specific type of **map** resulting from the projection of the satellite locations from the **satellite hemisphere** (horizontal coordinates) to a **plane** centred on the **user's location**

A network of **Ionospheric Scintillation Monitoring Receivers (ISMRs)** located in Brazil is exploited to generate high-density **ionospheric scintillation skyplots**



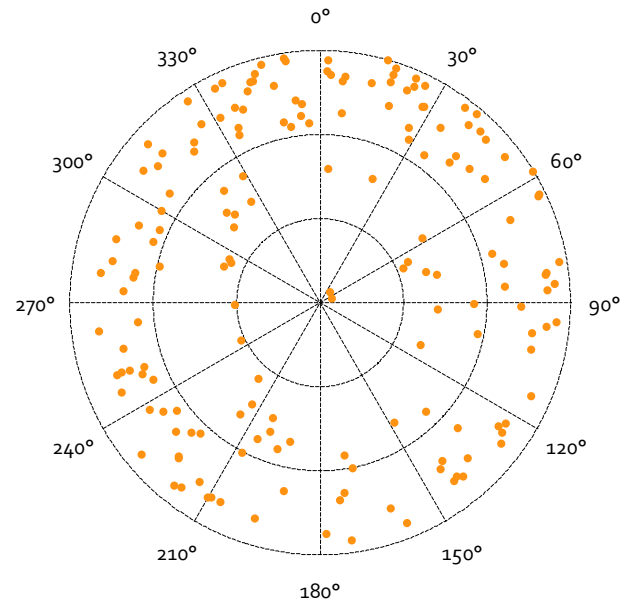
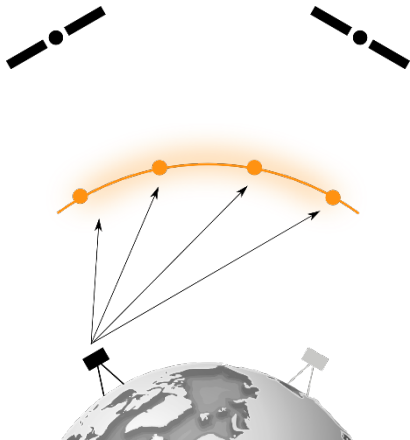
**Ionospheric Pierce Points (IPPs)** associated to satellite-receiver lines of sight related to a **network** of ISMRs can be exploited to generate **high-density skyplots**

A network of **Ionospheric Scintillation Monitoring Receivers (ISMRs)** located in Brazil is exploited to generate high-density **ionospheric scintillation skyplots**



**Ionospheric Pierce Points (IPPs)** associated to satellite-receiver lines of sight related to a **network** of ISMRs can be exploited to generate **high-density skyplots**

A network of **Ionospheric Scintillation Monitoring Receivers (ISMRs)** located in Brazil is exploited to generate high-density **ionospheric scintillation skyplots**



**Ionospheric Pierce Points (IPPs)** associated to satellite-receiver lines of sight related to a **network** of ISMRs can be exploited to generate **high-density skyplots**

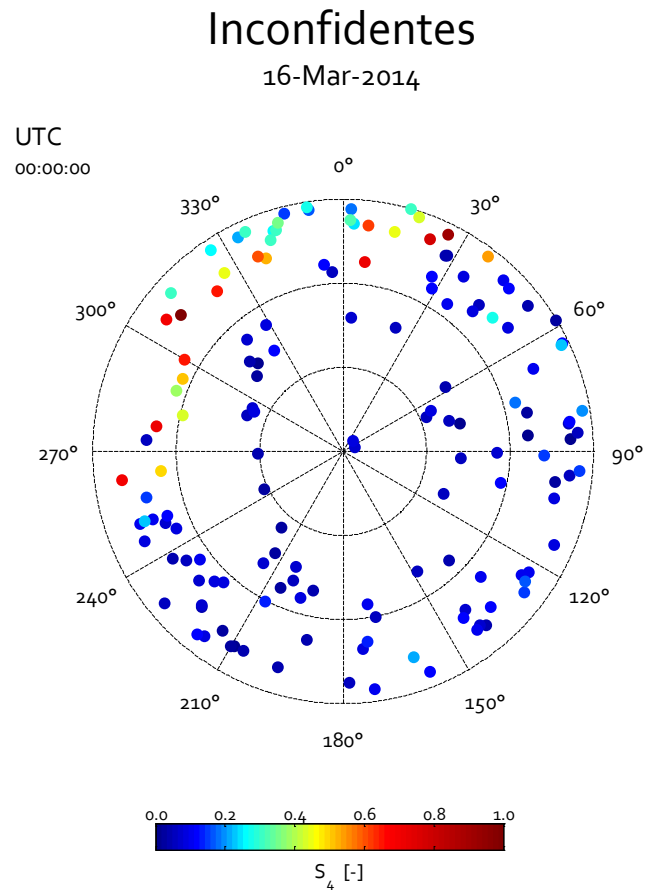
A network of **Ionospheric Scintillation Monitoring Receivers** (ISMRs) located in Brazil is exploited to generate high-density **ionospheric scintillation skyplots**

### Geometric Component

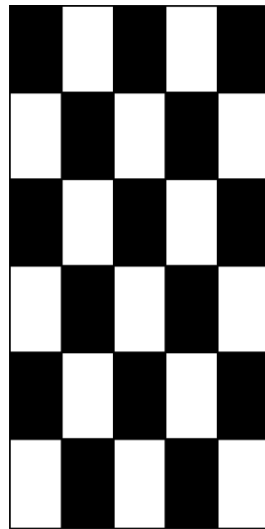
The locations of the IPPs depend on the GNSS orbits and the geographic coordinates of the user's location

### Attribute Component

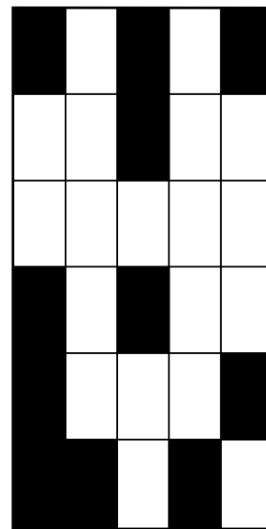
The values of the  $S_4$  index for every IPP depends on the instantaneous state of the ionosphere



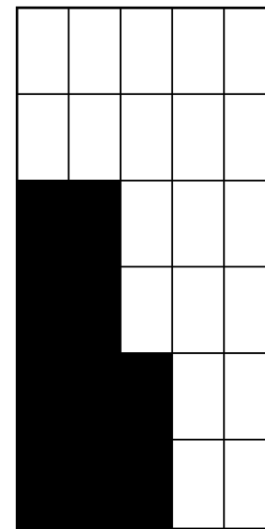
Spatial Autocorrelation constitutes a measure of how similar are nearby objects



Negative SAC



Neutral SAC



Positive SAC

Positive SAC is essential to compute interpolated maps



Detection → Scaling → Tracking

Spatial Autocorrelation **indices** can be calculated and **statistically tested** to **detect** the presence of significantly positive spatial autocorrelation in a given scatter plot

**Moran's I**  
Index

$$I = \frac{N}{S_0} \frac{\sum_{i=1}^N \sum_{j=1}^N w_{ij} (z_i - \bar{z})(z_j - \bar{z})}{\sum_{i=1}^N z_i^2}$$

**Geary's C**  
Index

$$C = \frac{(N-1)}{2 S_0} \frac{\sum_{i=1}^N \sum_{j=1}^N w_{ij} (z_i - z_j)^2}{\sum_{i=1}^N (z_i - \bar{z})^2}$$

**Getis-Ord General G**  
Statistic

$$G = \frac{\sum_{i=1}^N \sum_{j=1}^N w_{ij} z_i z_j}{\sum_{i=1}^N z_i z_j}$$

$$S_0 = \sum_{i=1}^N \sum_{j=1}^N w_{ij}$$

$$w_{ij} = \begin{cases} \frac{1}{d_{ij}^2}, & i \neq j \\ 0, & i = j \end{cases}$$

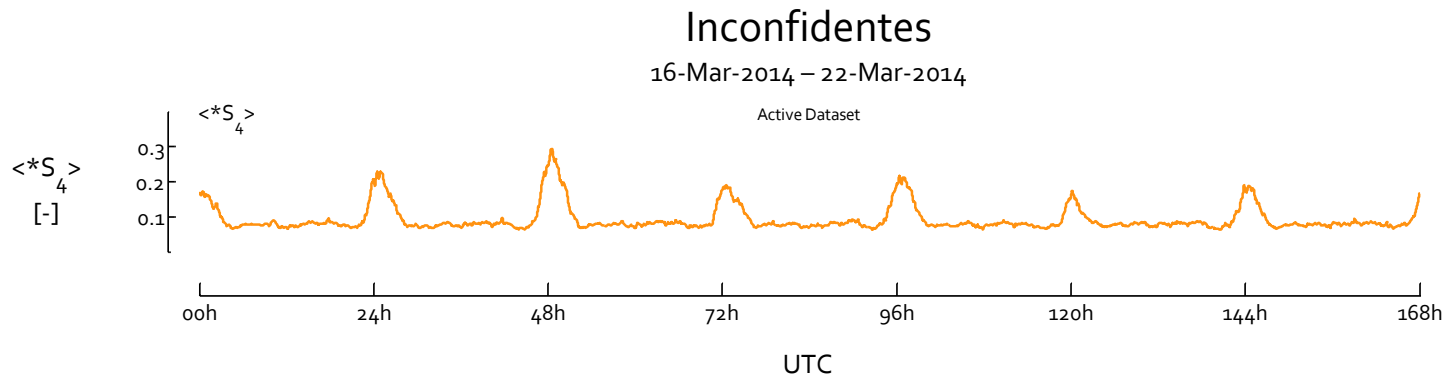
SAC indices are based on the geometric and attribute components of Ionospheric Scintillation Skyplots

SAC indices consider all possible pairs of entities

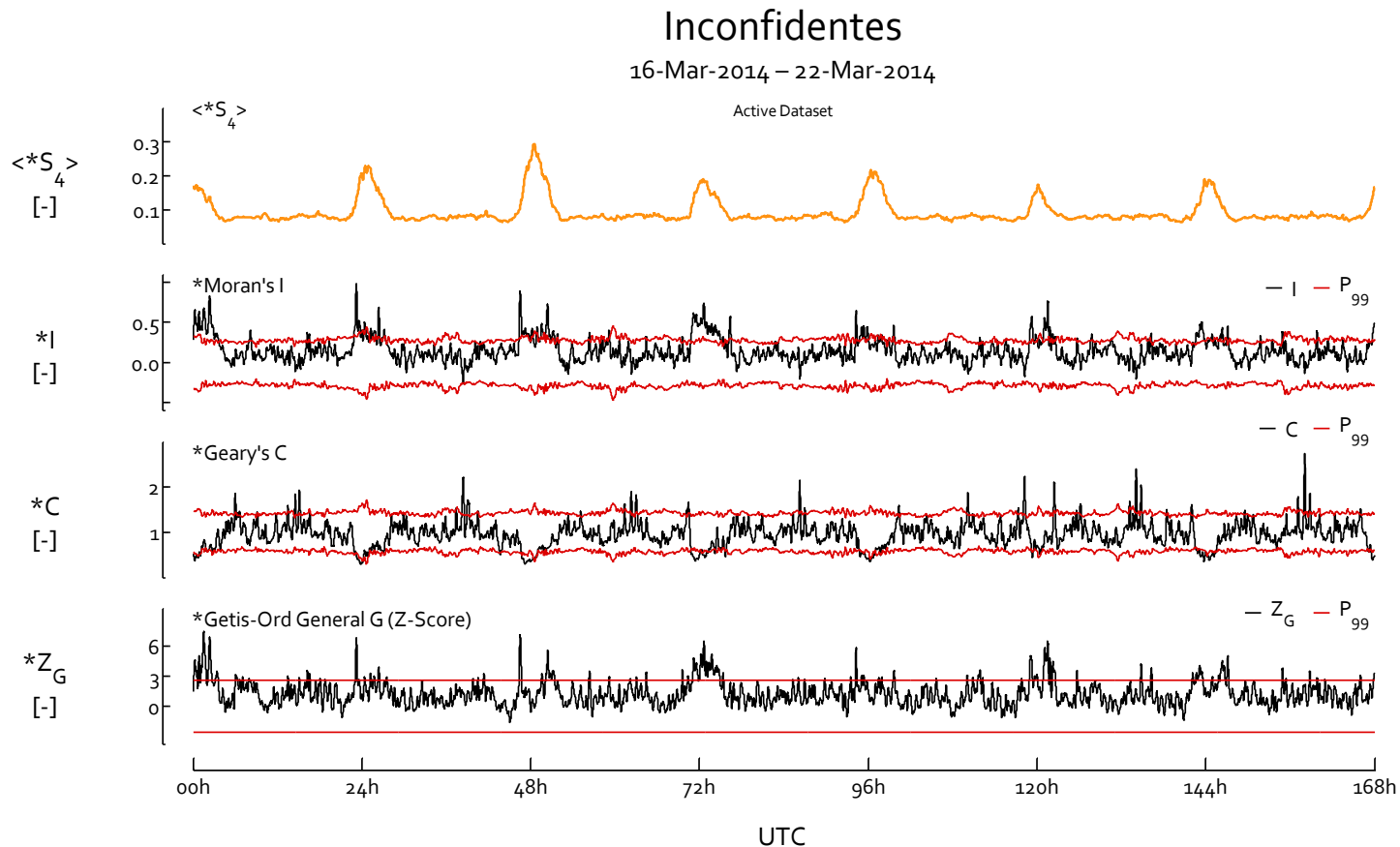
SAC indices are based on a weight function based on the interdistance related to each pair of entities



Ionospheric scintillation skyplots show significantly positive spatial autocorrelation during active ionospheric scintillation conditions at the station of Inconfidentes, Brazil



Ionospheric scintillation skyplots show **significantly positive spatial autocorrelation** during **active** ionospheric scintillation conditions at the station of **Inconfidentes**, Brazil



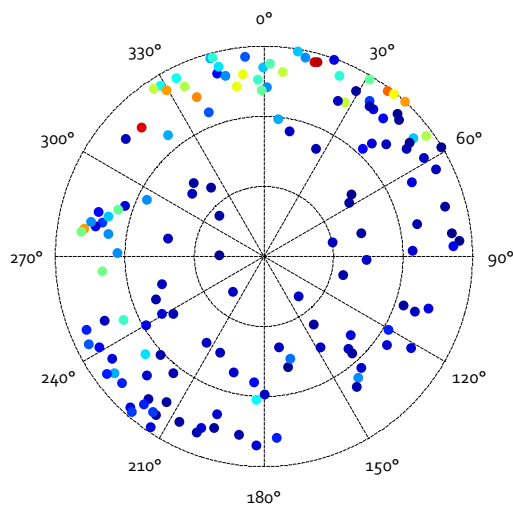
**Global SAC Indices** have specific characteristics which highlight their complementarity:

- |            |   |
|------------|---|
| Moran:     | Global SAC                                      |
| Geary:     | Global index with high sensitivity to Local SAC |
| Getis-Ord: | Clustering Index                                |

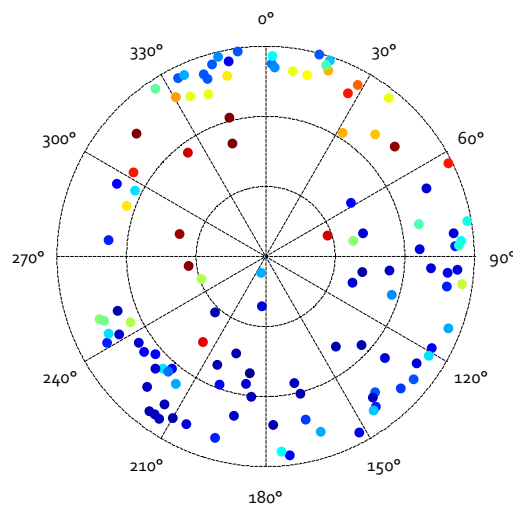
Ionospheric scintillation skyplots show **significantly positive spatial autocorrelation** during **active** ionospheric scintillation conditions at the station of **Inconfidentes**, Brazil

## Inconfidentes

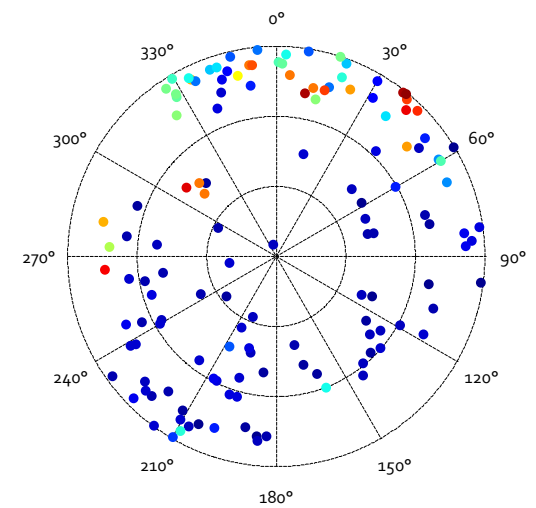
16-Mar-2014 – 22-Mar-2014



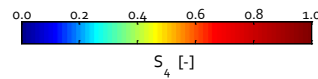
**CS<sub>1</sub>**  
Moran's I Index



**CS<sub>2</sub>**  
Geary's C Index



**CS<sub>3</sub>**  
Getis-Ord General G Statistic



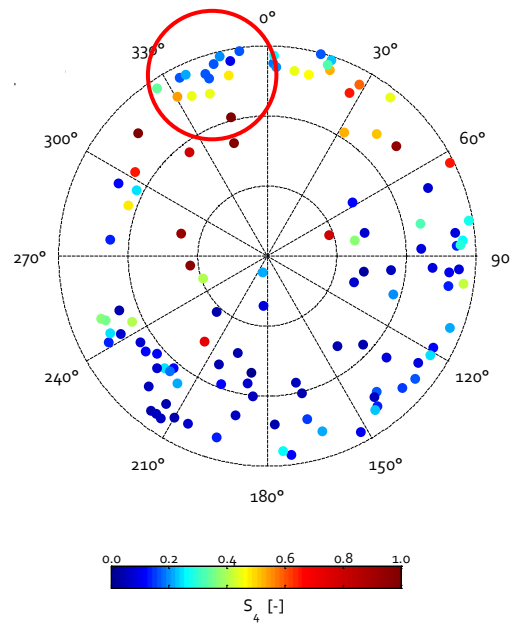
The **tracking** of spatial features impacting the global spatial autocorrelation is performed by exploiting **local** versions of the **spatial autocorrelation indices**

Size of the convolution window

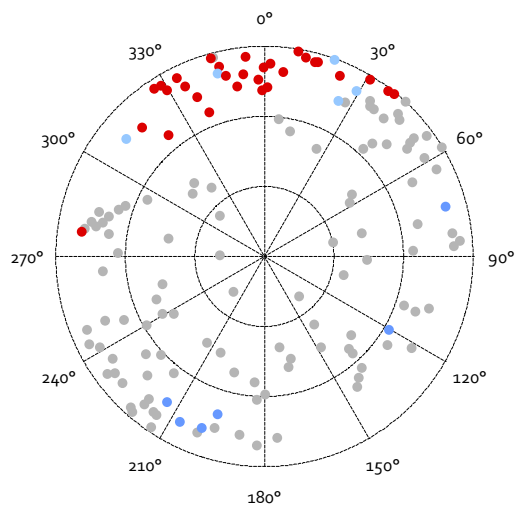
**20°**

Significance level

**95%**

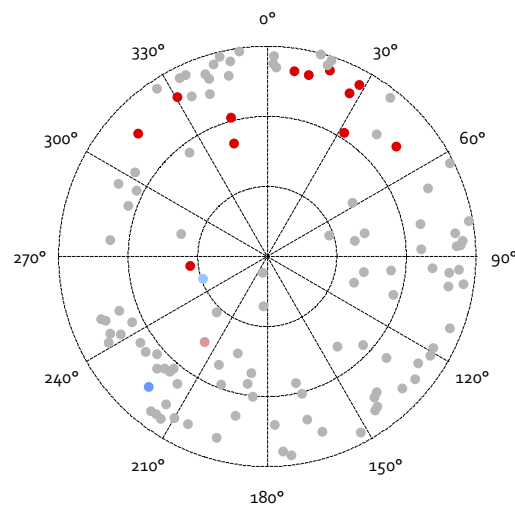


The **tracking** of spatial features impacting the global spatial autocorrelation is performed by exploiting **local** versions of the **spatial autocorrelation indices**



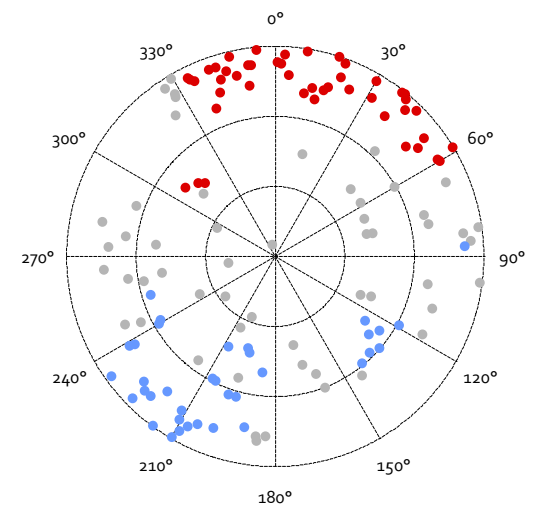
● High/High ● Low/Low ● High/Low ● Low/High

**CS<sub>1</sub>**  
Moran's I Index



● High/High ● Low/Low ● High/Low ● Low/High

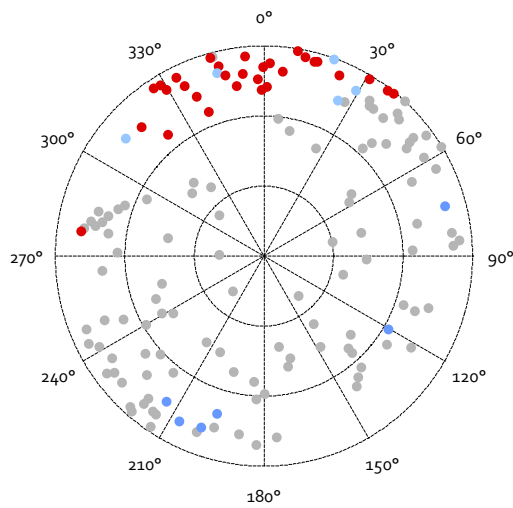
**CS<sub>2</sub>**  
Geary's C Index



● High/High ● Low/Low

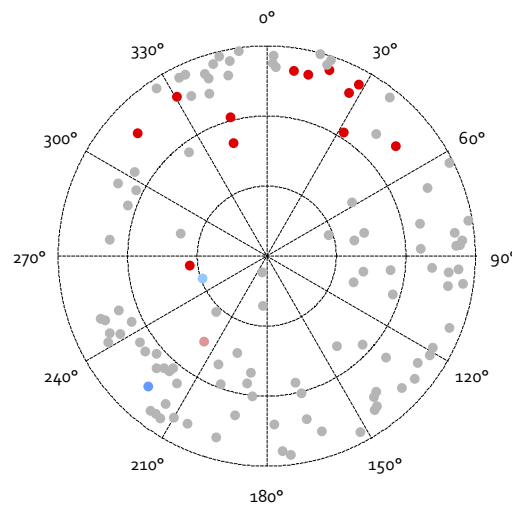
**CS<sub>3</sub>**  
Getis-Ord  $G_i^*$  Index

The **tracking** of spatial features impacting the global spatial autocorrelation is performed by exploiting **local** versions of the **spatial autocorrelation indices**



● High/High ● Low/Low ● High/Low ● Low/High

**CS<sub>1</sub>**  
Moran's I Index



● High/High ● Low/Low ● High/Low ● Low/High

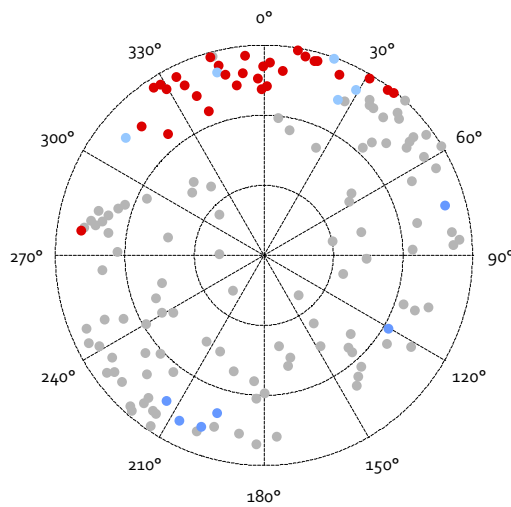
**CS<sub>2</sub>**  
Geary's C Index

$$G_i^*(d_k) = \frac{\sum_{j=1}^N w_{ij} z_j}{\sum_{j=1}^N z_j}$$

$$w_{ij} = \begin{cases} \frac{1}{d_{ij}^2}, & i \neq j \\ 0, & i = j \end{cases}$$

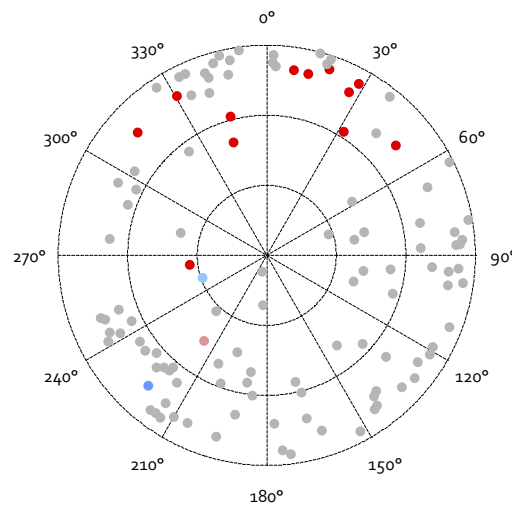
**CS<sub>3</sub>**  
Getis-Ord  $G_i^*$  Index

The **tracking** of spatial features impacting the global spatial autocorrelation is performed by exploiting **local** versions of the **spatial autocorrelation indices**



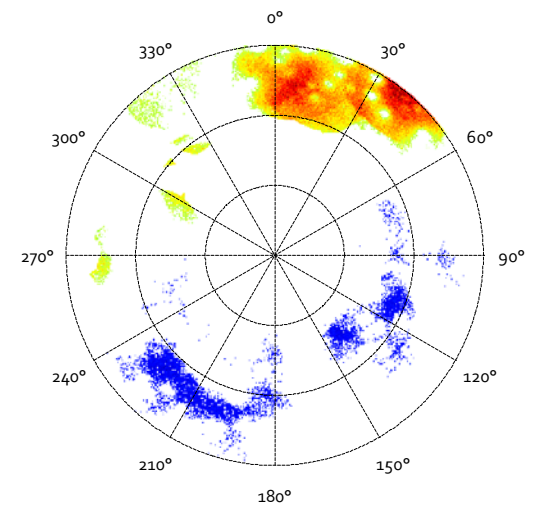
● High/High ● Low/Low ● High/Low ● Low/High

**CS<sub>1</sub>**  
Moran's I Index



● High/High ● Low/Low ● High/Low ● Low/High

**CS<sub>2</sub>**  
Geary's C Index



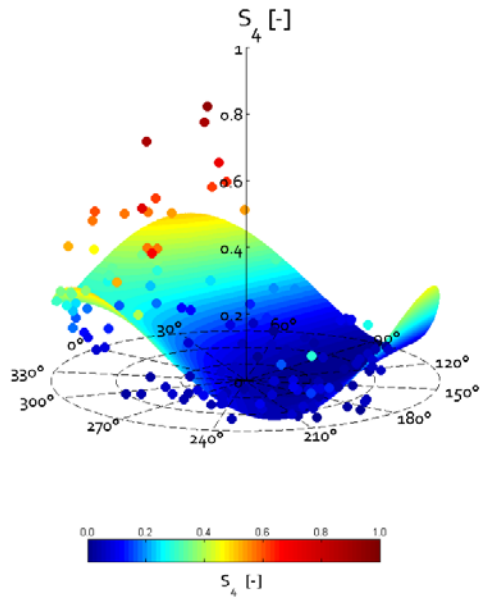
$Z_G [-]$

A horizontal color scale ranging from -3 to 6. The scale is labeled with -3, 0, 3, and 6. The colors transition from dark blue at -3, through light blue, green, yellow, and orange, to dark red at 6.

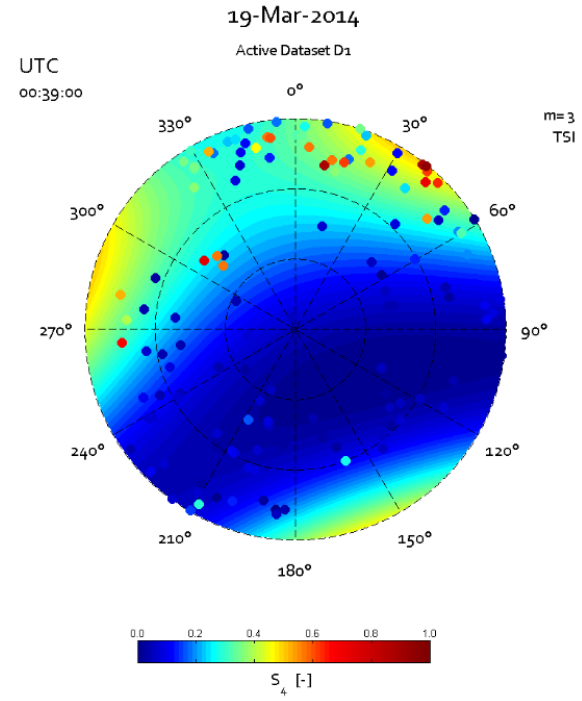
**CS<sub>3</sub>**  
Getis-Ord  $G_i^*$  Index

Local and global spatial autocorrelation in ionospheric scintillation skyplots can also be exploited by specific techniques to generate interpolated maps

### TSI – Trend Surface Interpolation



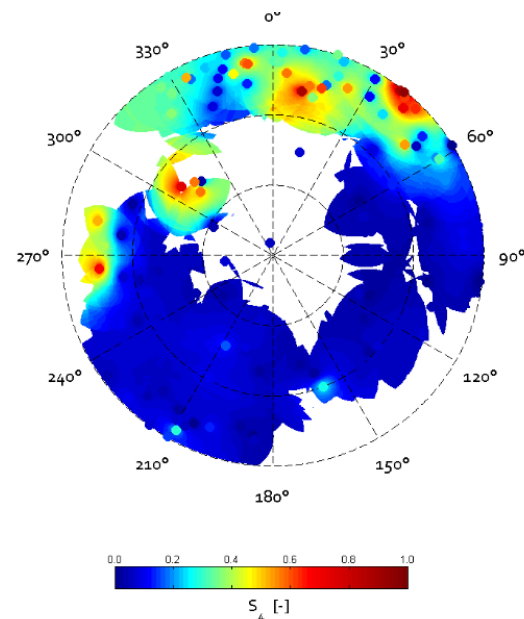
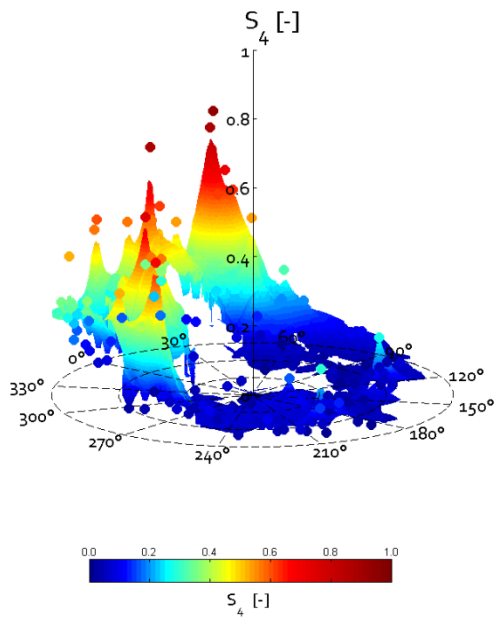
### Inconfidentes





Local and global spatial autocorrelation in ionospheric scintillation skyplots can also be exploited by specific techniques to generate interpolated maps

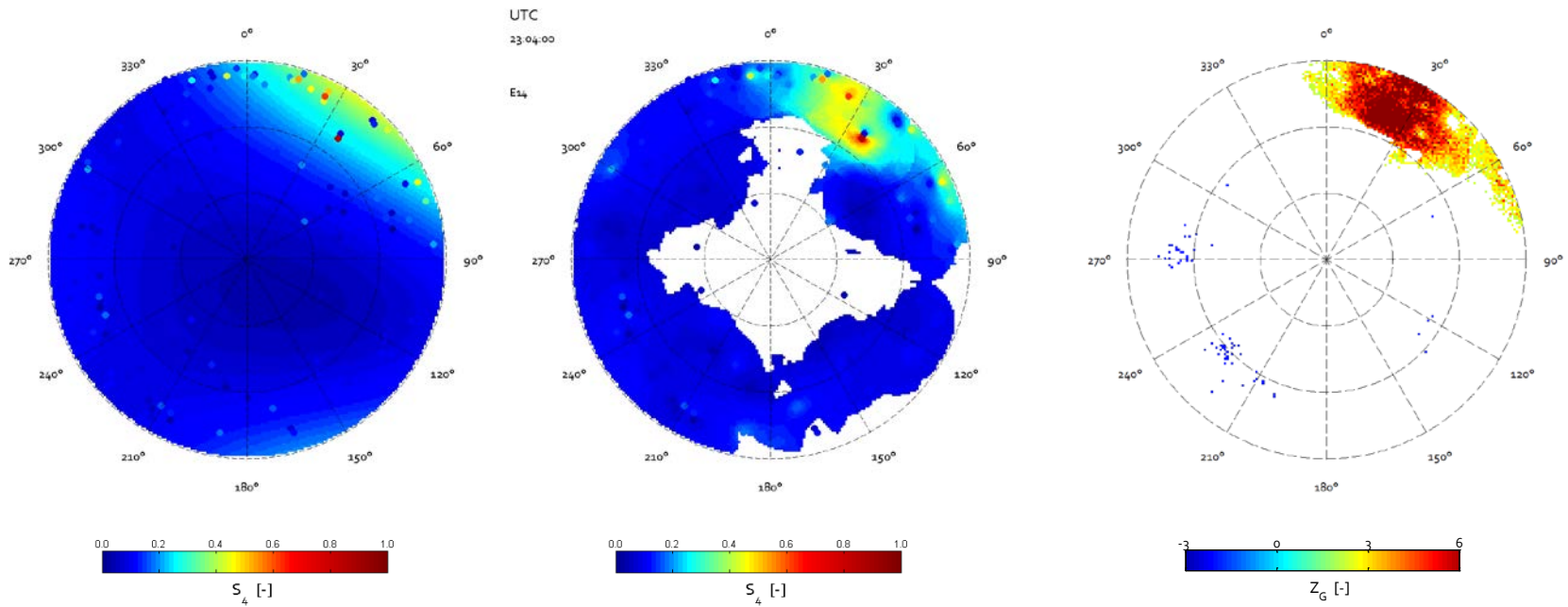
### IDW – Inverse Distance Weighting



Spatial analysis techniques applied to ionospheric scintillation skyplots can be exploited to generate three types of spatial products / ionospheric scintillation skymaps

## Inconfidentes

18-Mar-2014 – 19-Mar-2014



TSI skymaps

IDW skymaps

GOS skymaps

## Analysis

GNSS Algorithms and Ionosphere

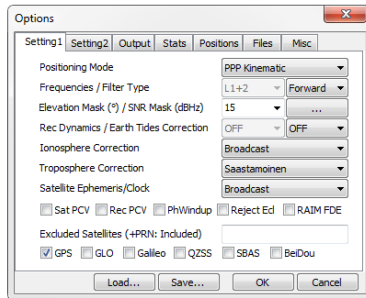
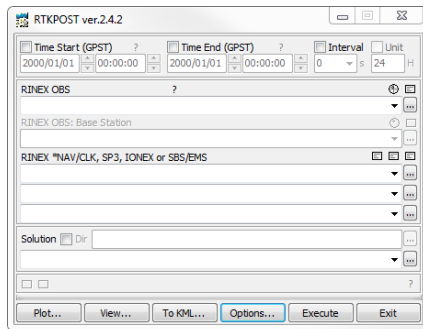
## Geostatistics

Ionospheric Scintillation Skymaps

## Prototypes

Mitigation Strategies

The **prototyping** of mitigation strategies against ionospheric scintillations is grafted to the post-processing **GNSS software RTKLIB**



**RTKLIB**

## Workspace

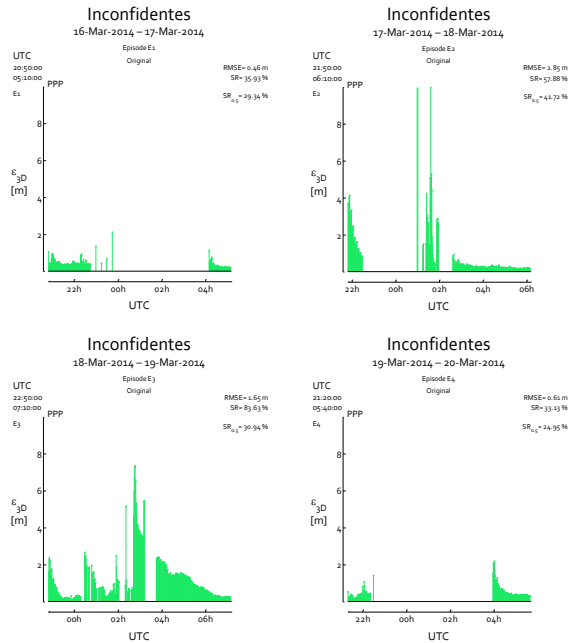
Post-processing GNSS Software RTKLIB

SPP and PPP Algorithms

Multiple Constellations (GPS, GLONASS, Galileo)

Open-Source code (C language)

Mitigation strategies against ionospheric scintillations are benchmarked at the ISMR station of **Inconfidentes**, Brazil, during **four** specific **6h-long** ionospheric scintillation **episodes**



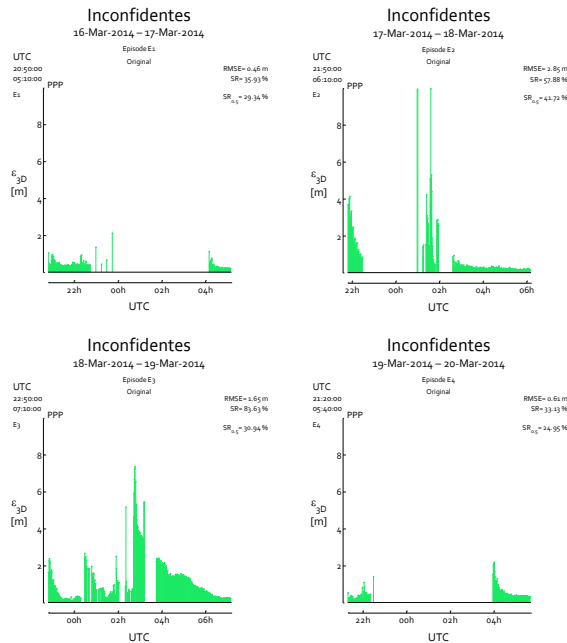
## Workspace

Post-processing GNSS Software RTKLIB

ISMR station of Inconfidentes, Brazil

Experimental Episodes E1/E2/E3/E4

The **benchmark** of the prototype mitigation strategies against ionospheric scintillations requires the definition of several **performance criteria**



## Workspace

Post-processing GNSS Software RTKLIB

ISMR station of Inconfidentes, Brazil

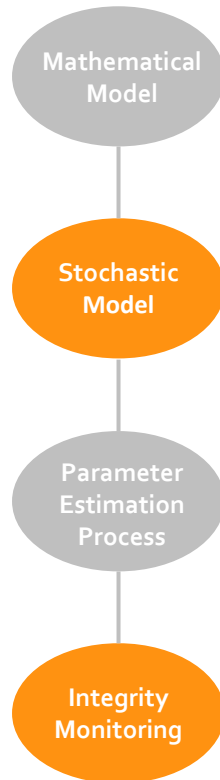
Experimental Episodes E1/E2/E3/E4

## Performance Criteria

- ➔ Accuracy      Root-Mean-Square Error (**RMSE**)
- ➔ Continuity      Success Rate (**SR**)
- ➔ Reliability      Success Rate for a given accuracy (**SR<sub>xx</sub>**)

Processing Time

Prototype mitigation strategies target the **stochastic modelling** stage and the **integrity monitoring** stage of the **SPP** and **PPP** algorithms



### Workspace

Post-processing GNSS Software RTKLIB

ISMR station of Inconfidentes, Brazil

Experimental Episodes E1/E2/E3/E4

Performance Criteria

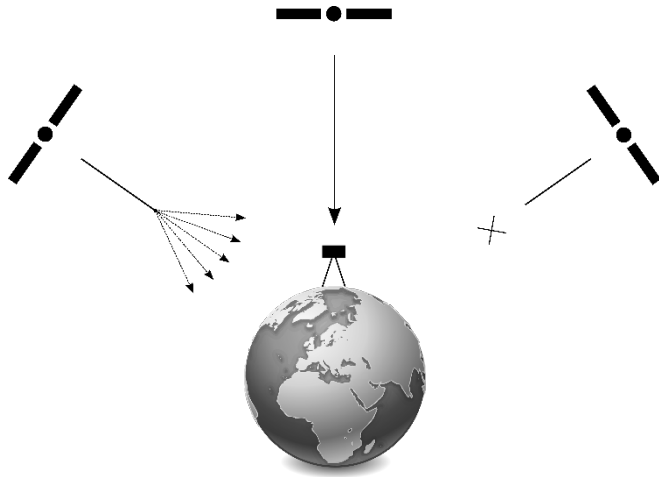
Targets

→ Stochastic Modelling

→ Integrity Monitoring

→ SPP/PPP Algorithms

The **stochastic model** of the **SPP/PPP** algorithms is represented by the **covariance matrix** of the **observations** which contains information related to the precision of the individual **measurements**



### Covariance Matrix of the Observations

$$Q_l = \sigma^2 I_m = \begin{bmatrix} \sigma^{1^2} & & & \\ & \sigma^{2^2} & & \\ & & \ddots & \\ & & & \sigma^{m^2} \end{bmatrix}$$

Two approaches are considered to customise the stochastic model of the SPP and PPP Algorithms

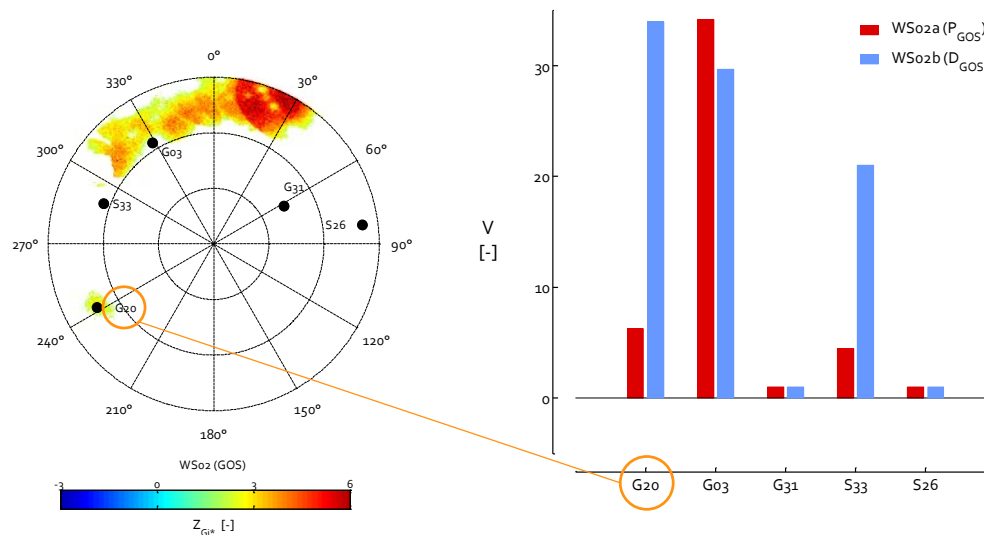
Weighting Scheme (WS)

Spatial Masks (SM)



The **Weighting Scheme (WS)** of the **stochastic model** can be tuned by adjusting calibrated **stochastic factors** based on ionospheric scintillation **skymaps** to **deweight** culprit observations

A **Calibration Process** based on the actual tracking variance (Conker Model) is exploited in order to defined the variation of the **Stochastic Factors** according to variables measurable in skymaps

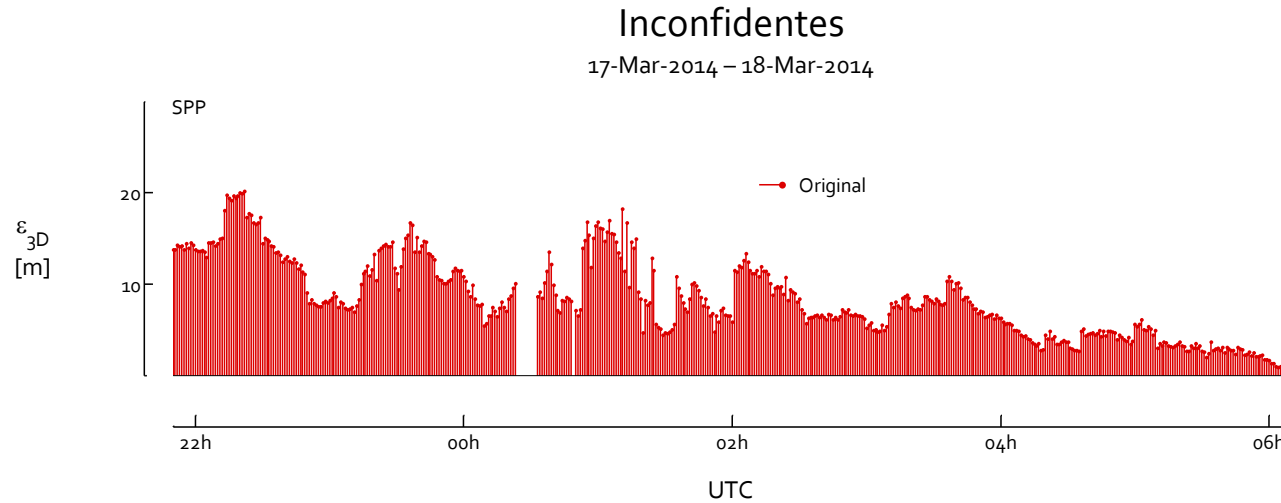


$$\sigma^2 = \left[ F_{GNSS}^2 R^2 \left( a^2 + \frac{b^2}{\sin \eta^s} \right) \right] * V + \dots$$

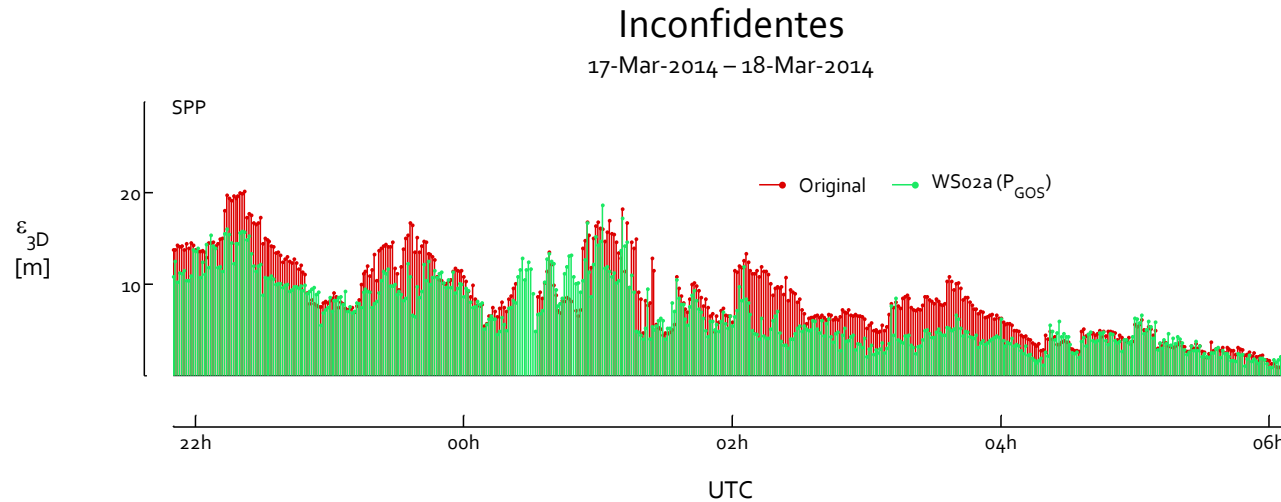
↑
↑

Tracking Variance
Stochastic Factor

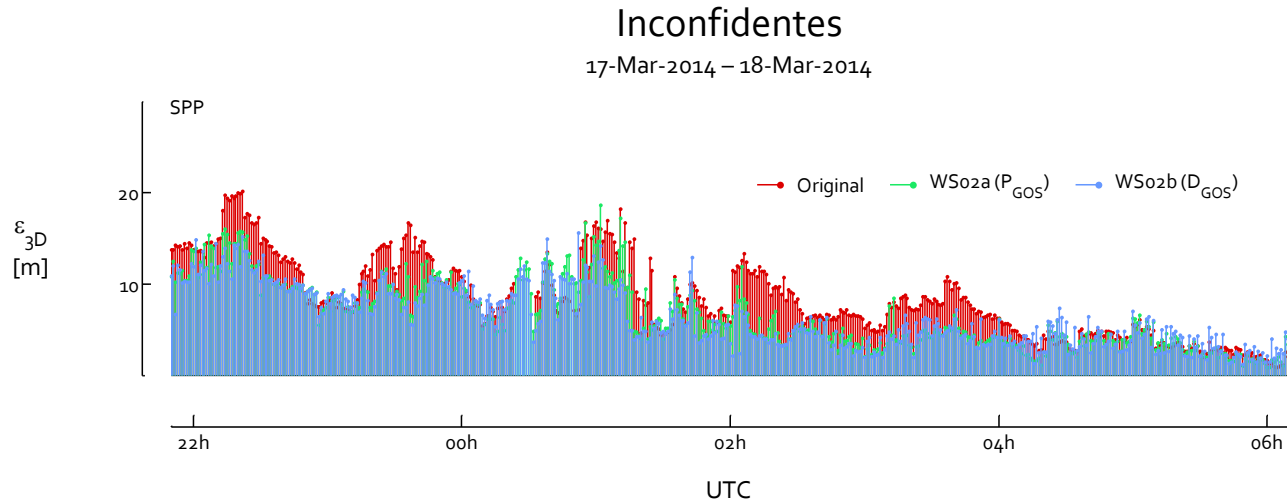
The **Weighting Scheme (WS)** of the **stochastic model** can be tuned by adjusting calibrated **stochastic factors** based on ionospheric scintillation **skymaps** to **deweight** culprit observations



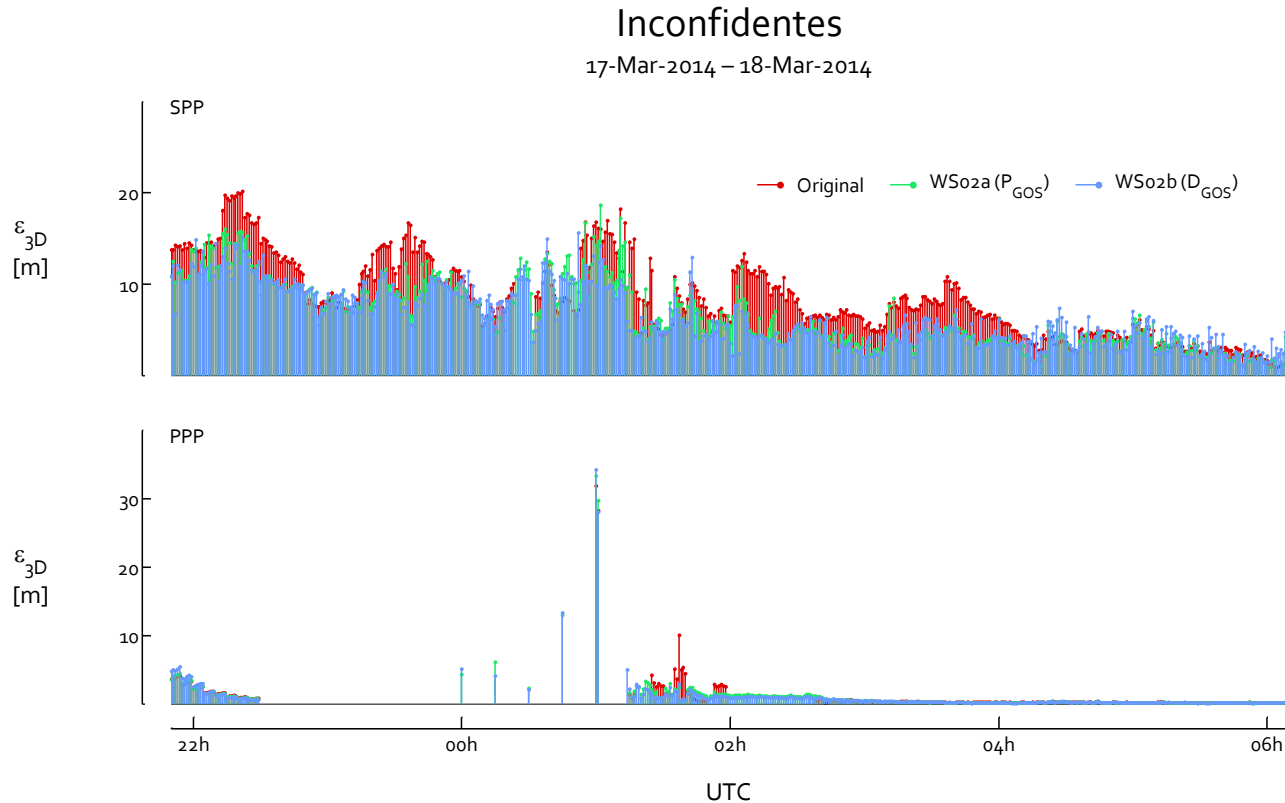
The **Weighting Scheme (WS)** of the **stochastic model** can be tuned by adjusting calibrated **stochastic factors** based on ionospheric scintillation **skymaps** to **deweight** culprit observations



The **Weighting Scheme (WS)** of the **stochastic model** can be tuned by adjusting calibrated **stochastic factors** based on ionospheric scintillation **skymaps** to **deweight** culprit observations

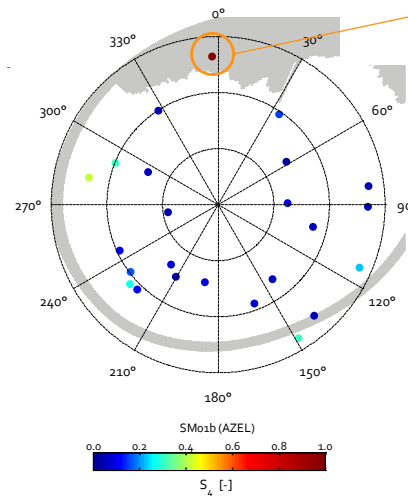
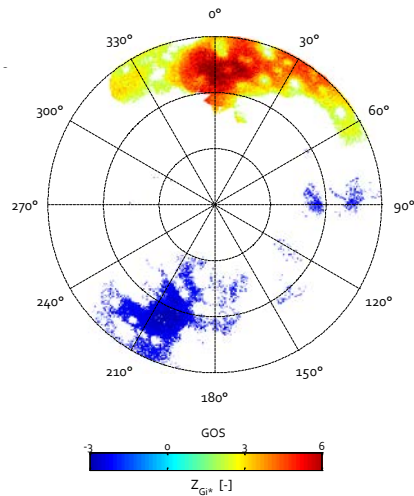


The **Weighting Scheme (WS)** of the **stochastic model** can be tuned by adjusting calibrated **stochastic factors** based on ionospheric scintillation **skymaps** to **deweight** culprit observations



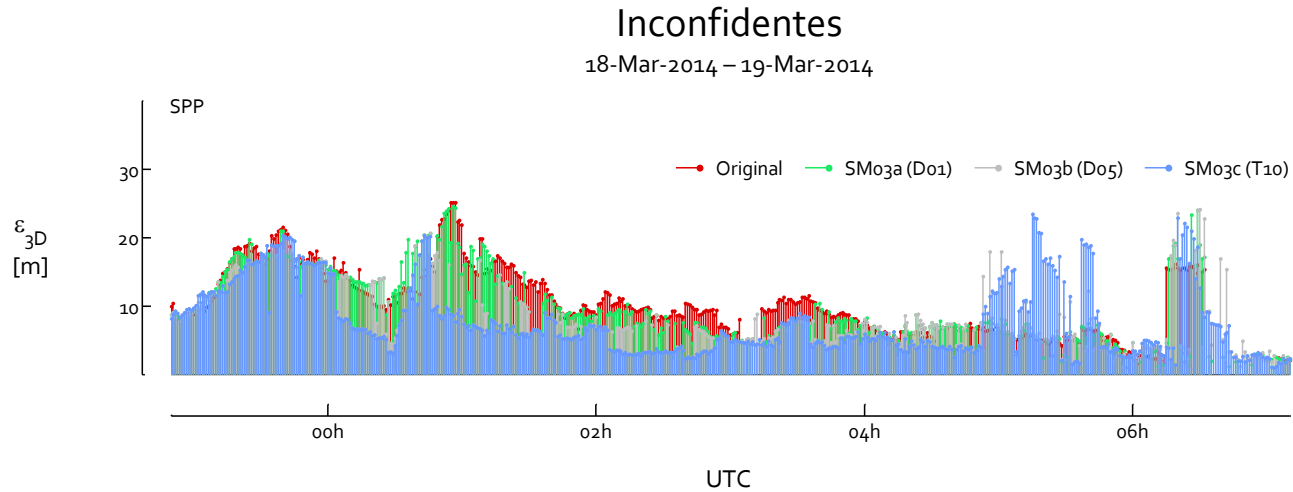
**Spatial Masks (SM)** are designed according to ionospheric scintillation **skymaps** in order to **exclude** potentially culprit observations from the parameter estimation process of the **SPP** and **PPP** algorithms

Ionospheric Scintillation Skymaps are exploited to design specific masks based on **various criteria**.

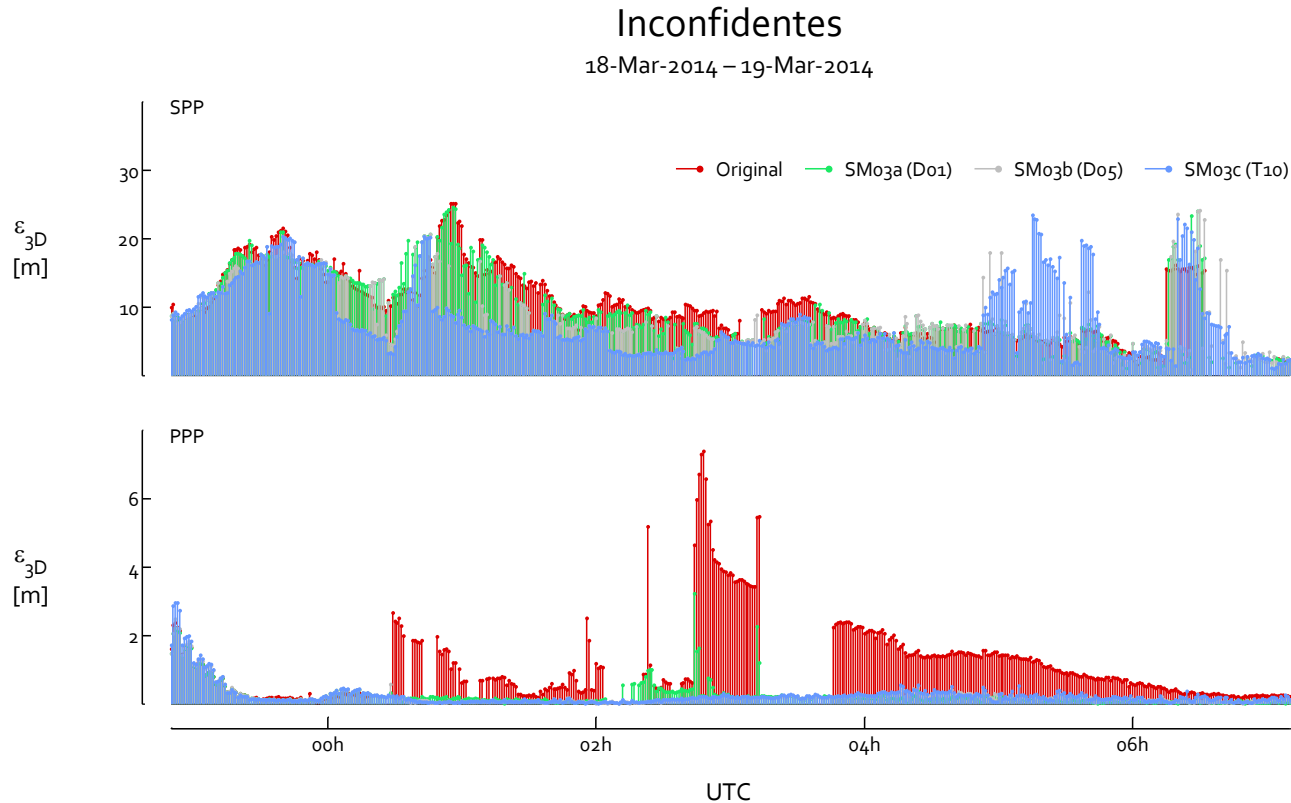


$$Q_L = \sigma^2 I_m = \begin{bmatrix} \sigma^{1^2} & \cancel{\sigma^{2^2}} & \dots \\ & & \sigma^{m^2} \end{bmatrix}$$

**Spatial Masks (SM)** are designed according to ionospheric scintillation **skymaps** in order to **exclude** potentially culprit observations from the parameter estimation process of the **SPP** and **PPP** algorithms



**Spatial Masks (SM)** are designed according to ionospheric scintillation **skymaps** in order to **exclude** potentially culprit observations from the parameter estimation process of the **SPP** and **PPP** algorithms





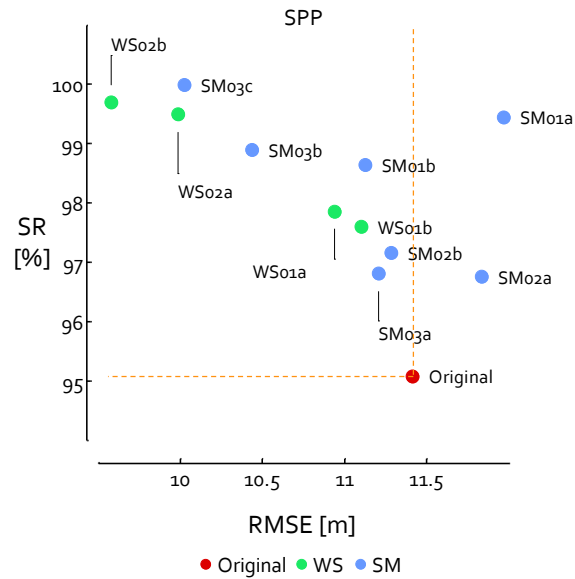
All prototype mitigation strategies increase the continuity of the SPP algorithm with a Success Rate ranging between 95% and 100%

## Inconfidentes

16-Mar-2014 – 20-Mar-2014

Experimental Episodes

E1-E2-E3-E4



All prototype mitigation strategies increase the continuity of the SPP algorithm with a Success Rate ranging between 95% and 100%

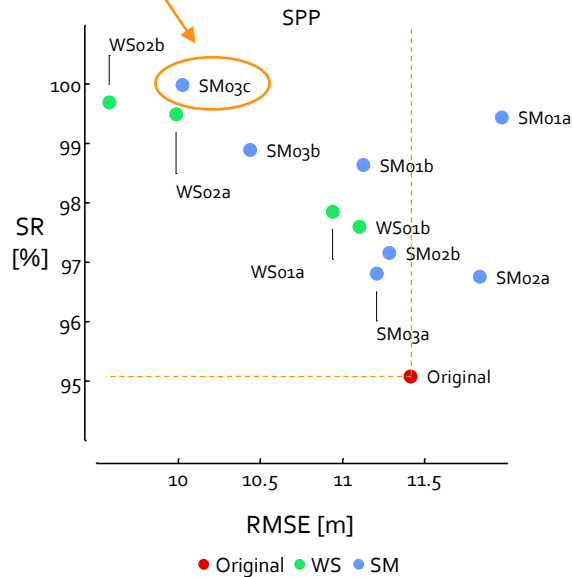
This mitigation strategy is based on a spatiotemporal buffer applied to GOS skymaps

## Inconfidentes

16-Mar-2014 – 20-Mar-2014

Experimental Episodes

E1-E2-E3-E4



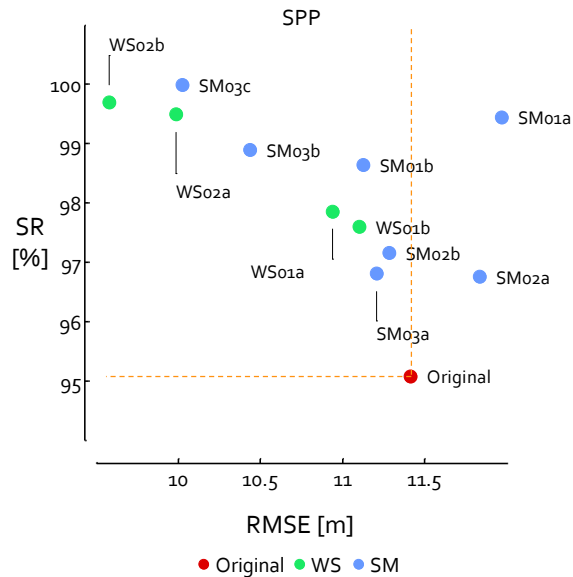
All prototype mitigation strategies increase the continuity of the SPP algorithm with a Success Rate ranging between 95% and 100%

## Inconfidentes

16-Mar-2014 – 20-Mar-2014

Experimental Episodes

E1-E2-E3-E4



The continuity of the SPP algorithm is always improved

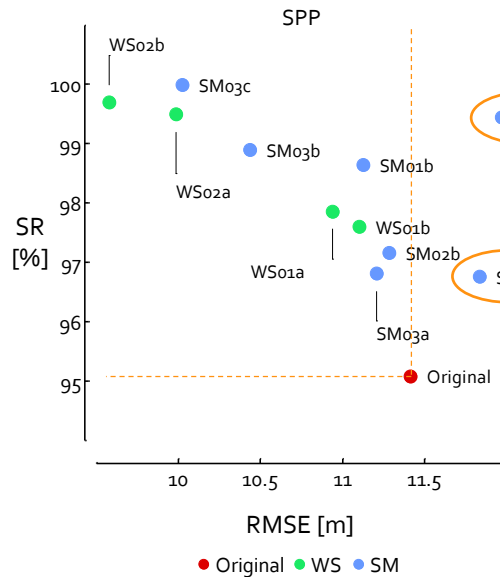
Almost all prototype mitigation strategies increase the accuracy of the SPP algorithm with an RMSE dropping from ~11m down to ~10m

## Inconfidentes

16-Mar-2014 – 20-Mar-2014

Experimental Episodes

E1-E2-E3-E4



The continuity of the SPP algorithm is always improved

Only those two strategies tend to decrease the accuracy of the SPP algorithm in case of ionospheric scintillations

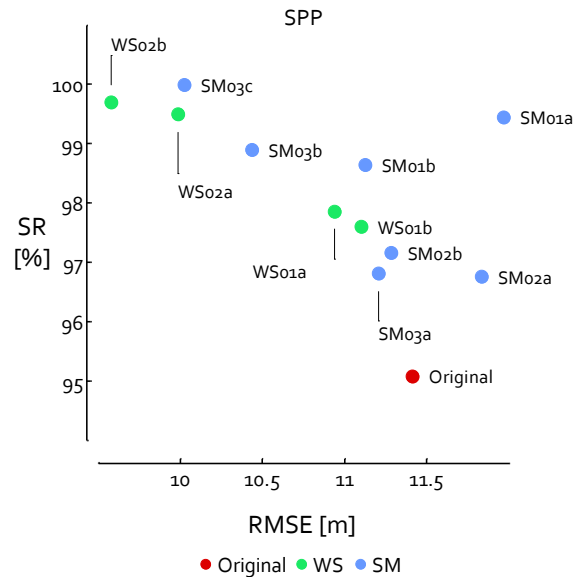
Almost all prototype mitigation strategies increase the accuracy of the SPP algorithm with an RMSE dropping from ~11m down to ~10m

## Inconfidentes

16-Mar-2014 – 20-Mar-2014

Experimental Episodes

E1-E2-E3-E4



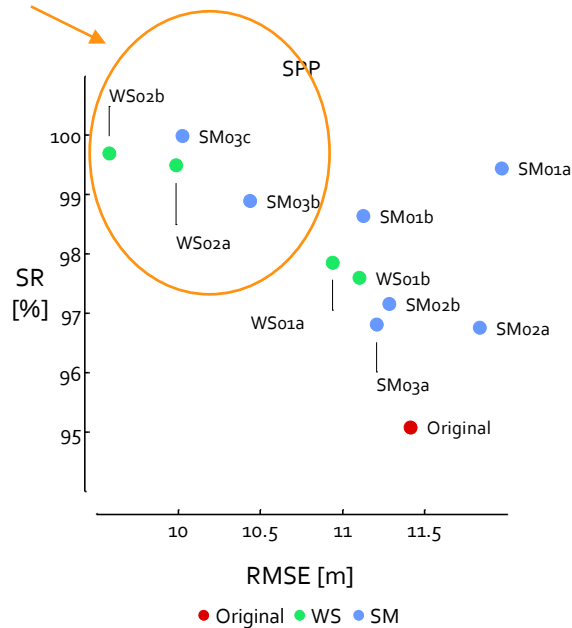
The continuity of the SPP algorithm is always improved

The accuracy of the SPP algorithm is improved by almost all the prototype mitigation strategies

Abusive spatial masks tend to decrease the quality of the satellite geometry

Prototype mitigation strategies based on **GOS skymaps** provide better **performances** which indicates a higher suitability of GOS skymaps for **GNSS positioning**

All those strategies are based on GOS skymaps



The continuity of the SPP algorithm is always improved

The accuracy of the SPP algorithm is improved by almost all the prototype mitigation strategies

Abusive spatial masks tend to decrease the quality of the satellite geometry

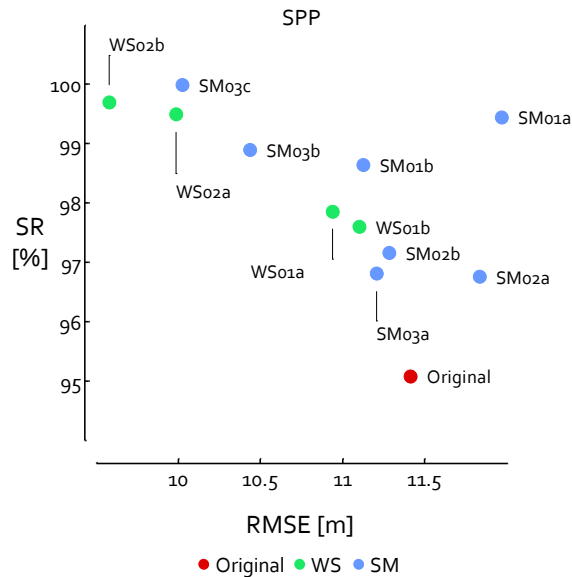
Prototype mitigation strategies based on **GOS skymaps** provide better **performances** which indicates a higher suitability of GOS skymaps for **GNSS positioning**

## Inconfidentes

16-Mar-2014 – 20-Mar-2014

Experimental Episodes

E1-E2-E3-E4



The continuity of the SPP algorithm is always improved

The accuracy of the SPP algorithm is improved by almost all the prototype mitigation strategies

Abusive spatial masks tend to decrease the quality of the satellite geometry

GOS Skymaps provide better results for GNSS positioning in terms of accuracy and continuity

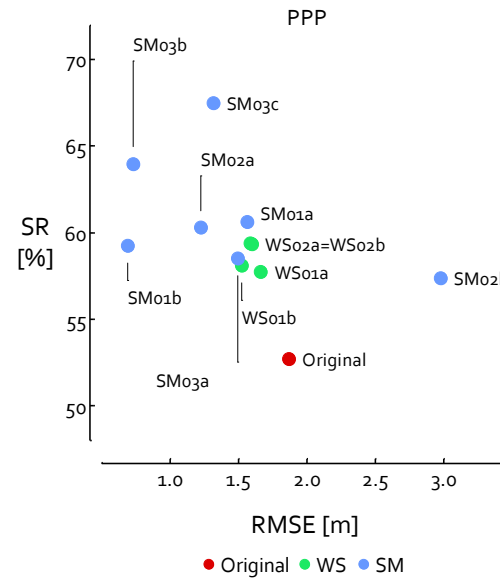
All prototype mitigation strategies increase the continuity of the PPP algorithm with a Success Rate ranging between ~52% and ~68%

## Inconfidentes

16-Mar-2014 – 20-Mar-2014

Experimental Episodes

E1-E2-E3-E4





All prototype mitigation strategies increase the continuity of the PPP algorithm with a Success Rate ranging between ~52% and ~68%

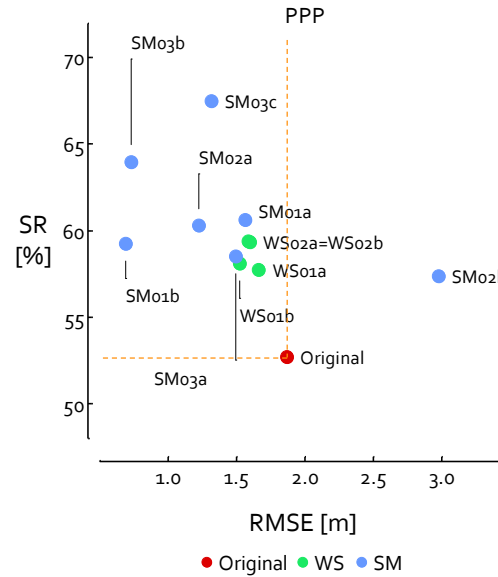
## Inconfidentes

16-Mar-2014 – 20-Mar-2014

Experimental Episodes

E1-E2-E3-E4

The continuity of the PPP Algorithm is always improved but it remains too low for demanding applications



All prototype mitigation strategies increase the continuity of the PPP algorithm with a Success Rate ranging between ~52% and ~68%

## Inconfidentes

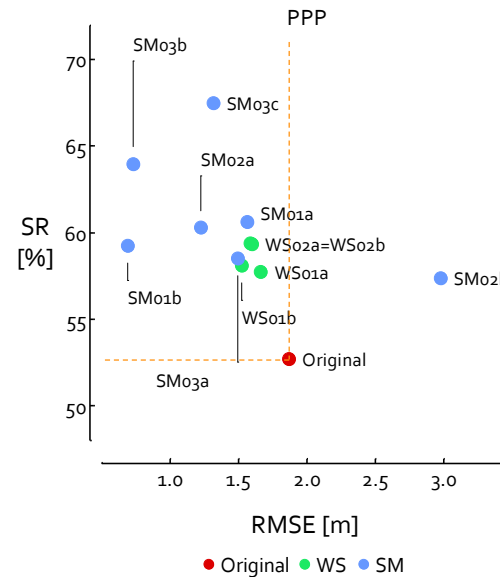
16-Mar-2014 – 20-Mar-2014

Experimental Episodes

E1-E2-E3-E4

The continuity of the PPP Algorithm is always improved but it remains too low for demanding applications

The accuracy performances of the PPP algorithm are improved but not to the expected level for the PPP algorithm



For the **PPP algorithm**, prototype mitigation strategies based on **spatial masks** provide better **performances** than strategies based on the tuning of the weighting scheme

## Inconfidentes

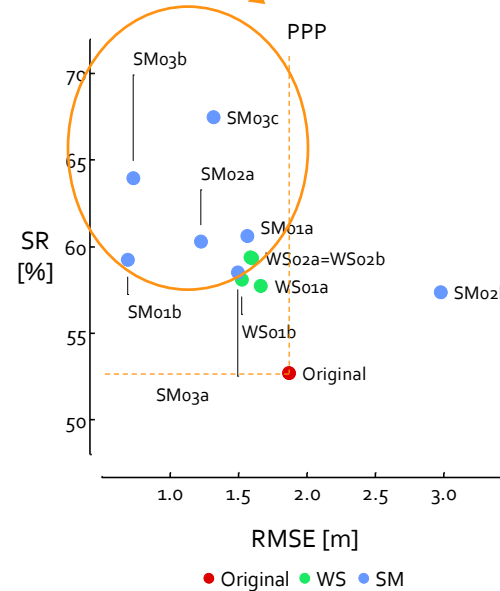
16-Mar-2014 – 20-Mar-2014

Experimental Episodes  
E1-E2-E3-E4

All those strategies  
are based on Spatial  
Masks

The continuity of the PPP Algorithm is always improved but it remains too low for demanding applications

The accuracy performances of the PPP algorithm are improved but not to the expected level for the PPP algorithm



For the **PPP algorithm**, prototype mitigation strategies based on **spatial masks** provide better **performances** than strategies based on the tuning of the weighting scheme

## Inconfidentes

16-Mar-2014 – 20-Mar-2014

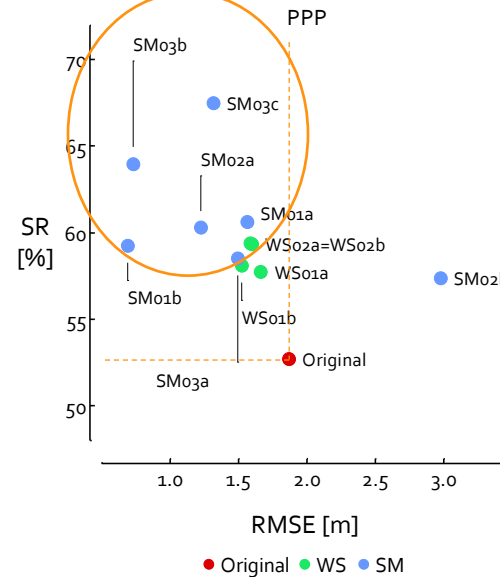
Experimental Episodes  
E1-E2-E3-E4

All those strategies  
are based on Spatial  
Masks

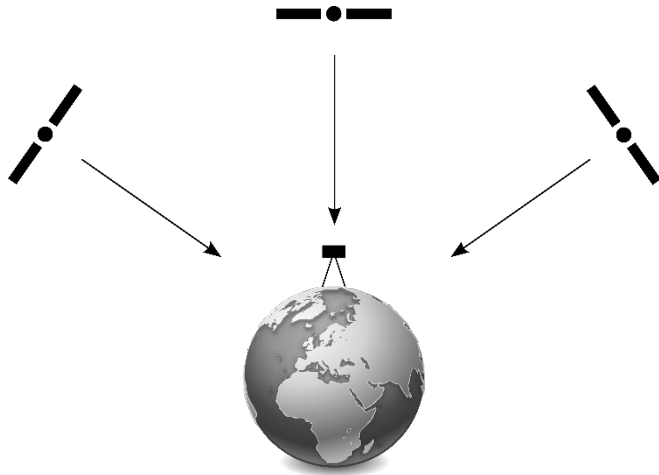
The continuity of the PPP Algorithm is always improved but it remains too low for demanding applications

The accuracy performances of the PPP algorithm are improved but not to the expected level for the PPP algorithm

For the PPP algorithm, designing spatial masks leads to better positioning performances than tuning the weighting scheme



The **integrity monitoring** stage of the **SPP** and **PPP** algorithms consists in statistically verifying the **validity** of the computed navigation **solution**



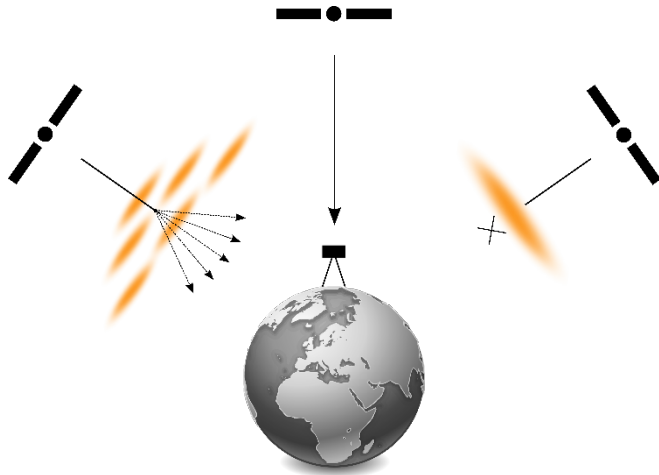
### Statistical Validation Test (RTKLIB)

$$v_r^s = \frac{[P_r^s - (\widehat{D}_r^s + c \widehat{dt}_r - c dt^s + I_r^s + T_r^s)]}{\sigma_{P_r^s}}$$

$$\underline{v} = (v_r^1, v_r^2, \dots, v_r^n)^T$$

$$\frac{\underline{v}^T W \underline{v}}{\sigma_0^2} < \chi_{\alpha}^2(n - m - 1)$$

The **integrity monitoring** stage of the **SPP** and **PPP** algorithms consists in statistically verifying the **validity** of the computed navigation **solution**



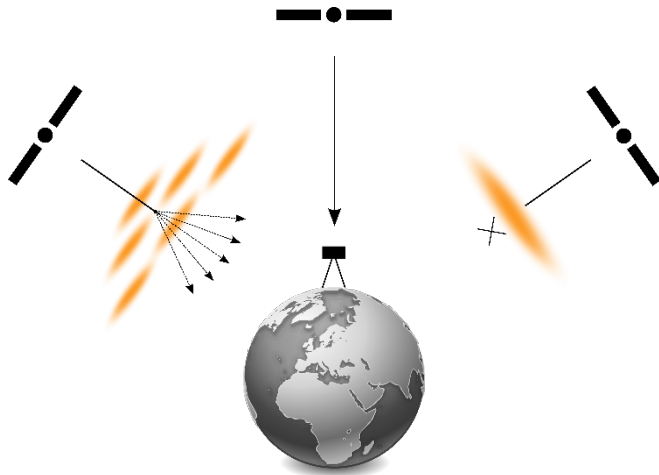
### Statistical Validation Test (RTKLIB)

$$v_r^s = \frac{[P_r^s - (\widehat{D}_r^s + c \widehat{dt}_r - c dt^s + I_r^s + T_r^s)]}{\sigma_{P_r^s}}$$

$$\underline{v} = (v_r^1, v_r^2, \dots, v_r^n)^T$$

$$\frac{\underline{v}^T W \underline{v}}{\sigma_0^2} < \chi_{\alpha}^2(n - m - 1)$$

The **integrity monitoring** stage of the **SPP** and **PPP** algorithms consists in statistically verifying the **validity** of the computed navigation **solution**



### Statistical Validation Test (RTKLIB)

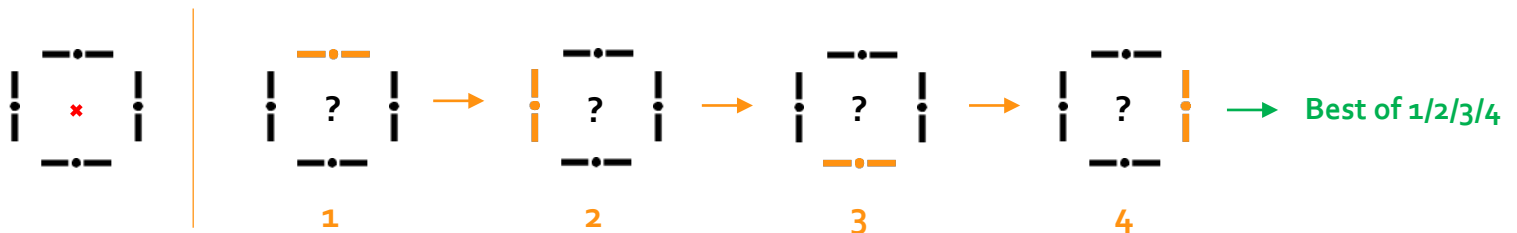
$$v_r^s = \frac{[P_r^s - (\widehat{D}_r^s + c \widehat{dt}_r - c dt^s + I_r^s + T_r^s)]}{\sigma_{P_r^s}}$$

$$\underline{v} = (v_r^1, v_r^2, \dots, v_r^n)^T$$

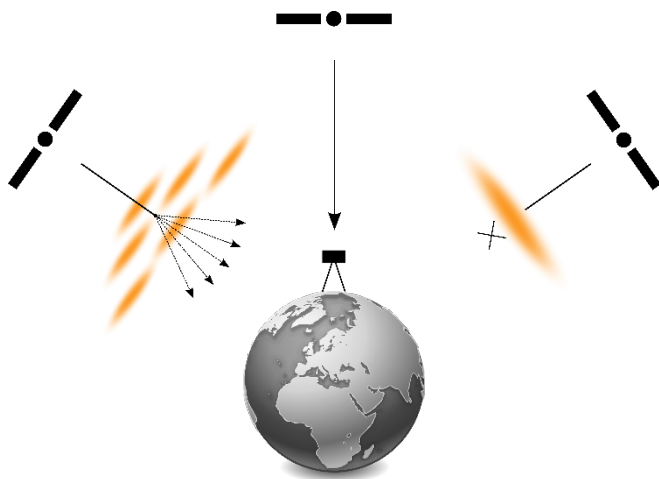
$$\frac{\underline{v}^T W \underline{v}}{\sigma_0^2} < \chi_\alpha^2(n - m - 1)$$

### RAIM-FDE

Receiver **A**utonomous **I**ntegrity **M**onitoring – **F**ault **D**etection **E**xclusion



The **integrity monitoring** stage of the **SPP** and **PPP** algorithms consists in statistically verifying the **validity** of the computed navigation **solution**



Three Approaches to design prototype mitigation strategies related to the integrity monitoring stage of the SPP and PPP Algorithms.

Original RTKLIB RAIM-FDE Technique (IMo0)

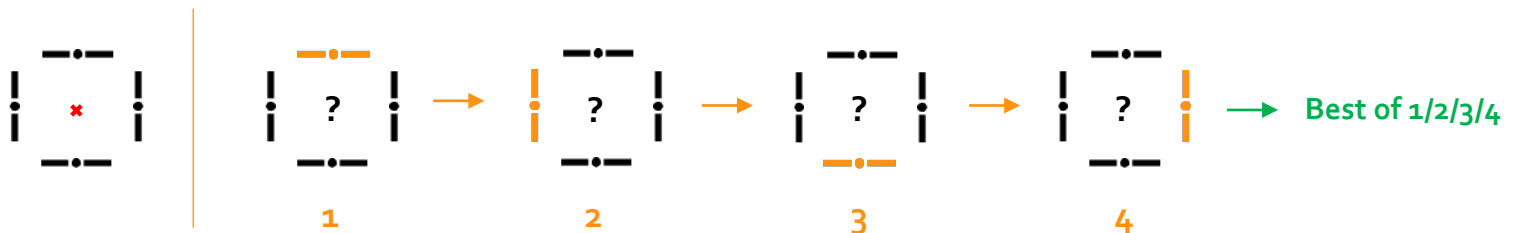
Extended Technique (IMo1)

Spatial Technique (IMo2)

Hybrid Solution (IMo3)

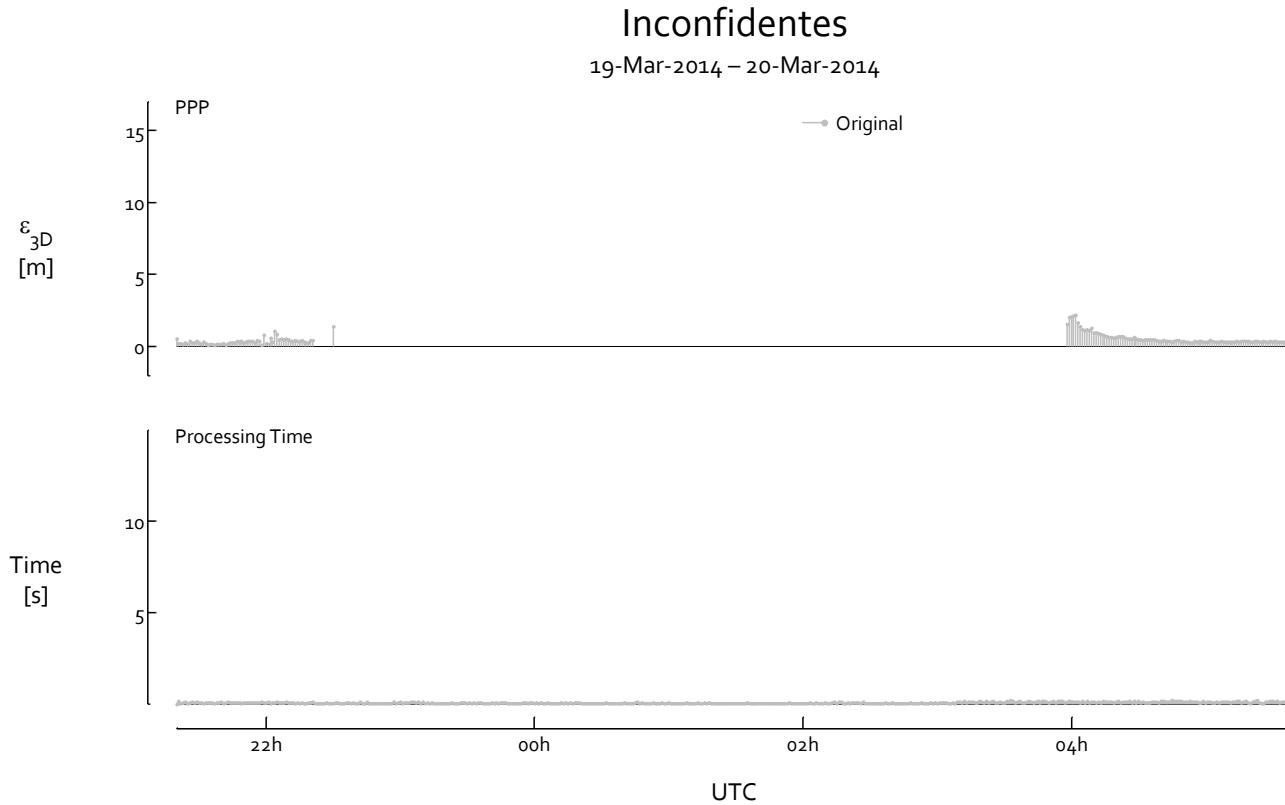
### RAIM-FDE

Receiver **A**utonomous **I**ntegrity **M**onitoring – **F**ault **D**etection **E**xclusion

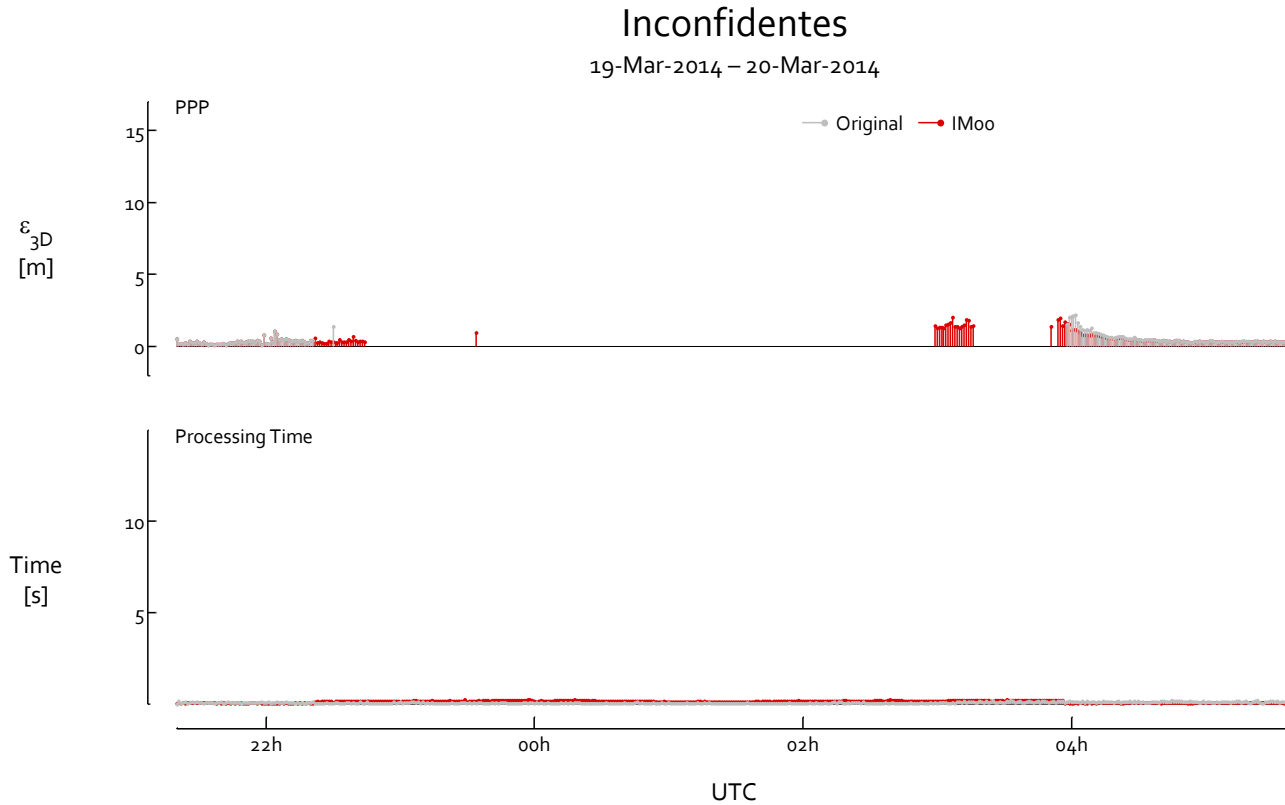




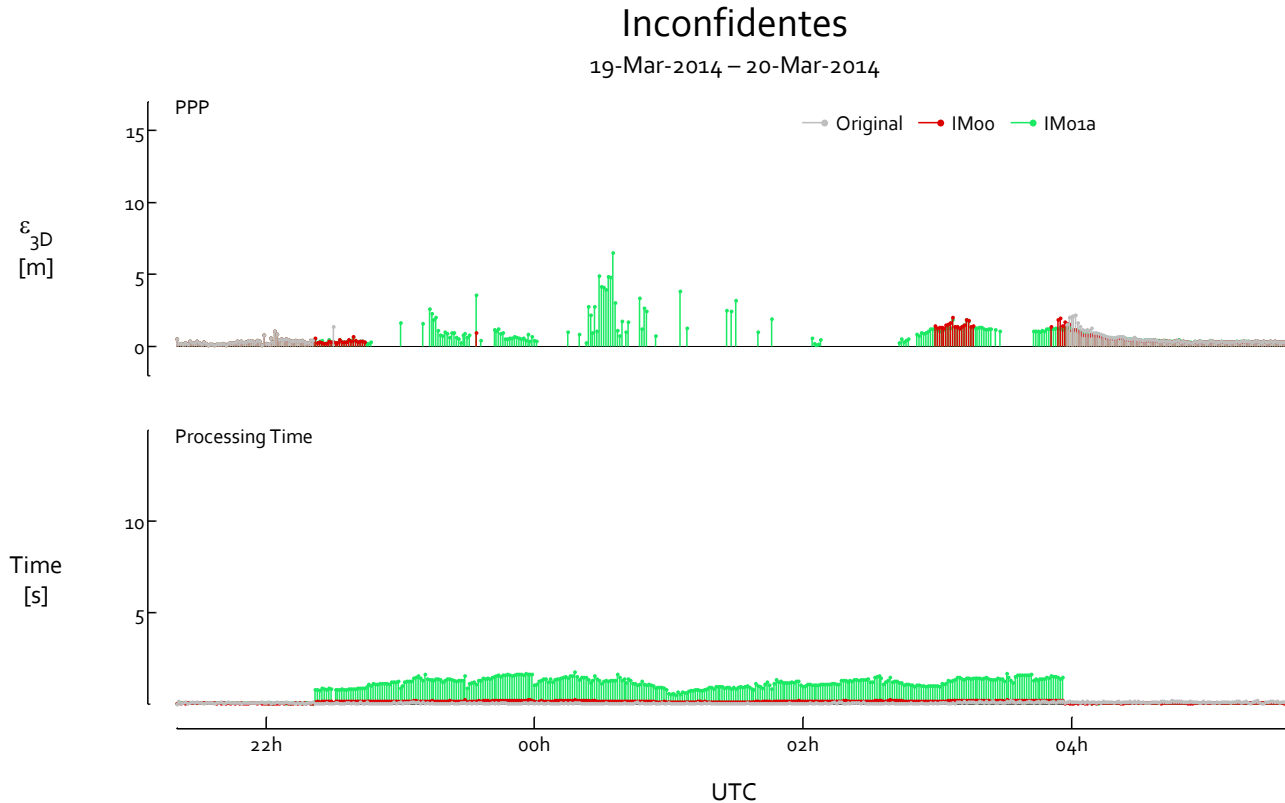
Advanced integrity monitoring is the key towards higher PPP performances in case of ionospheric scintillations but it requires a valid stochastic model



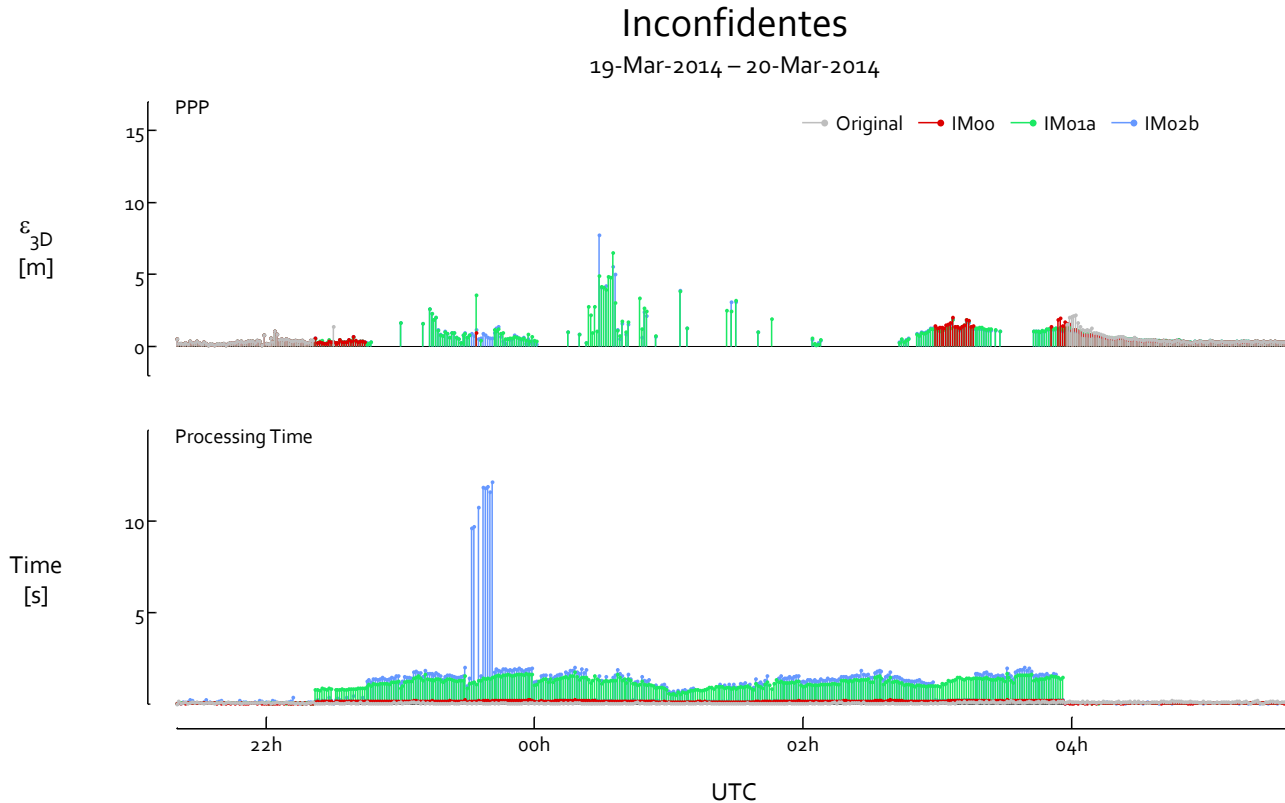
Advanced integrity monitoring is the key towards higher PPP performances in case of ionospheric scintillations but it requires a valid stochastic model



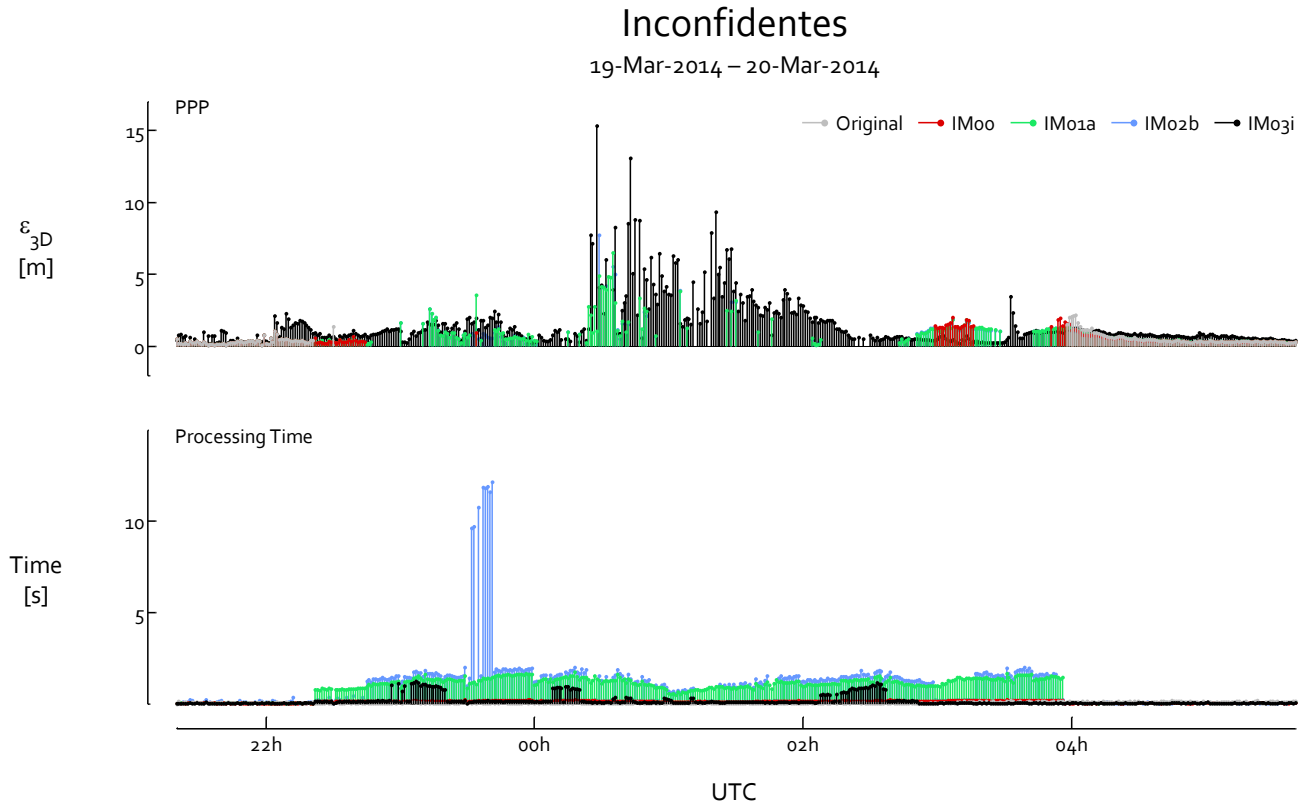
Advanced integrity monitoring is the key towards higher PPP performances in case of ionospheric scintillations but it requires a valid stochastic model



Advanced integrity monitoring is the key towards higher PPP performances in case of ionospheric scintillations but it requires a valid stochastic model



Advanced **integrity monitoring** is the key towards **higher PPP performances** in case of **ionospheric scintillations** but it requires a valid stochastic model



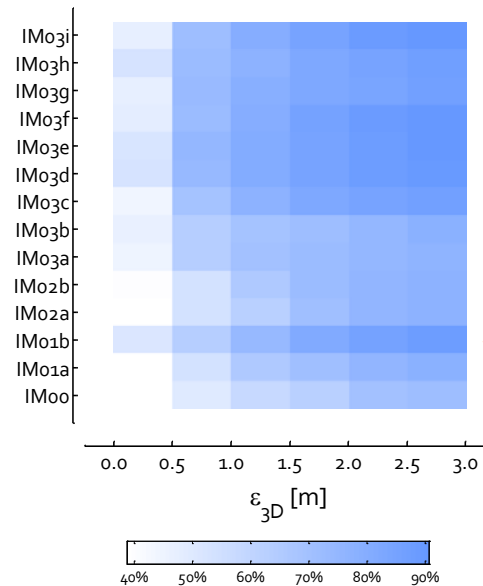
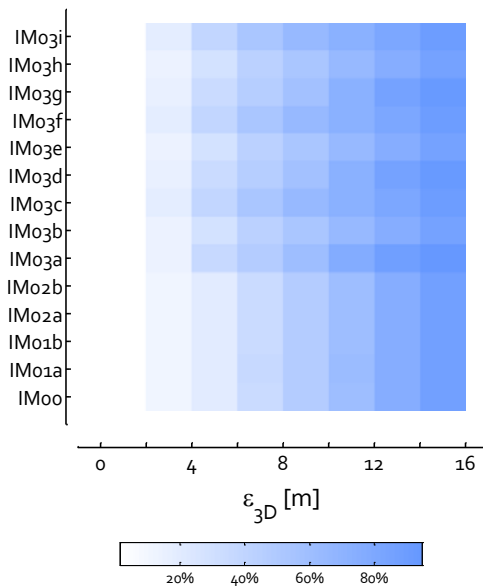
Hybrid prototype mitigation strategies targeting both the stochastic modelling and the integrity monitoring stages lead to the highest results for the SPP and PPP algorithms

## Inconfidentes

16-Mar-2014 – 20-Mar-2014

Experimental Episodes

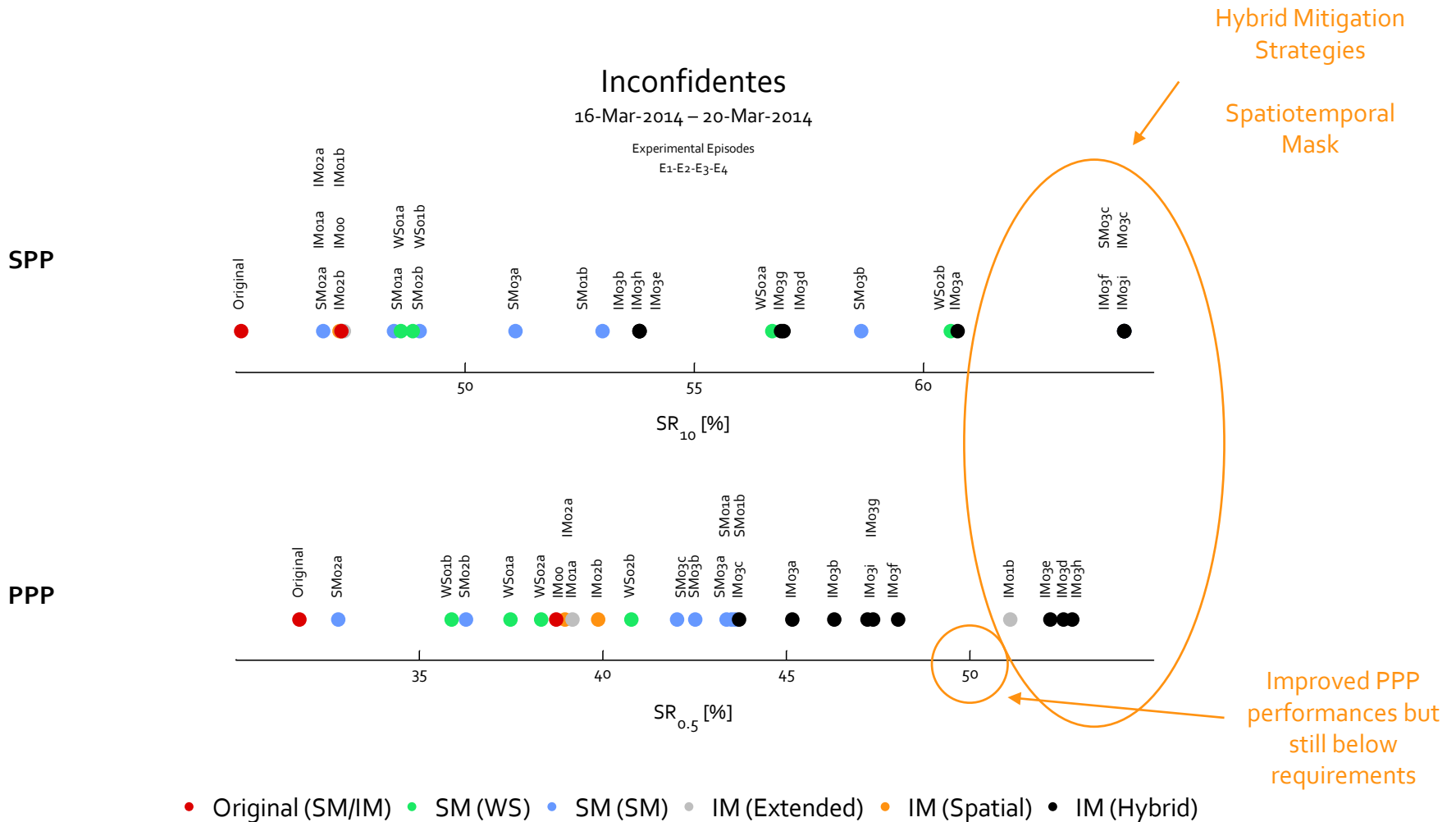
E1-E2-E3-E4



Hybrid Mitigation Strategies

Several exclusions systematically = very resource consuming

Hybrid prototype mitigation strategies targeting both the stochastic modelling and the integrity monitoring stages lead to the highest results for the SPP and PPP algorithms



## Analysis

GNSS Algorithms and Ionosphere

## Geostatistics

Ionospheric Scintillation Skymaps

## Prototypes

Mitigation Strategies



Spatial analysis techniques are applicable to GNSS/ISMR measurements collected in a network of stations located near the magnetic equator in order to produce real-time ionospheric scintillation skymaps (H1)

- Detection, scaling and tracking of spatial autocorrelation
- Real-time ionospheric scintillation skymaps

Mitigation strategies based on real-time ionospheric scintillation skymaps improve the performances of the SPP and PPP algorithms in case of low-latitude ionospheric scintillations (H2)

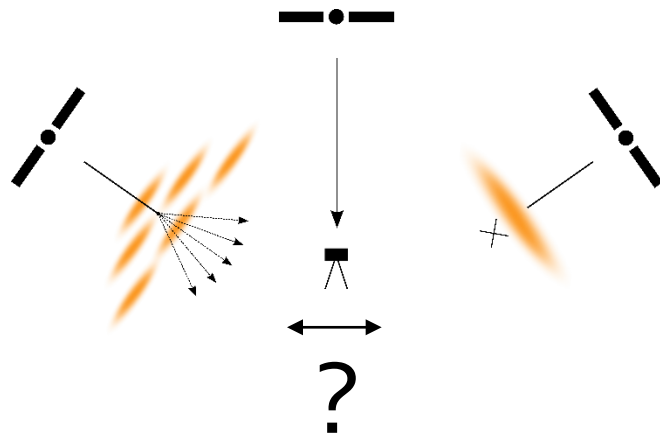
- General improvement of the accuracy, continuity and reliability of the SPP and PPP algorithms
- Higher reliability of the GOS skymaps
- SPP performances improved by tuning the weighting scheme of the stochastic model
- PPP performances improved by applying spatial masks
- Integrity monitoring can bring the performances to the next level in case of ionospheric scintillations
- Hybrid mitigation strategies are very powerful
- PPP performances remain below requirements during intense ionospheric scintillations at low latitudes  
 **$SR_{0.5} = 55\%$  max and at the cost of a heavy computational load**

...this research approach constitutes an encouraging breakthrough but there is still room for improvement!

## Perspectives exist to extend this research further and reach even better performances for GNSS positioning in case of ionospheric scintillations

- High-density ionospheric scintillation skymaps (space + time)
  - Alternative variables to measure the impact of ionospheric scintillations on GNSS signals
  - Multiple GNSS constellations
  - High-density GNSS/ISMR networks
  - Smartphone-based crowdsourcing
- Advanced RAIM-FDE technology combined with adaptive exclusion process (pre-processing) and stochastic model
  - GOS skymaps
  - Individual testing
  - Phase/Code/Doppler validation tests
  - Adaptive computational load
- High-latitude ionospheric scintillations
- Application of the approach in other harsh tracking environment (jamming, multipath, etc.)

# Ingestion of Ionospheric Scintillation Skymaps into GNSS Algorithms



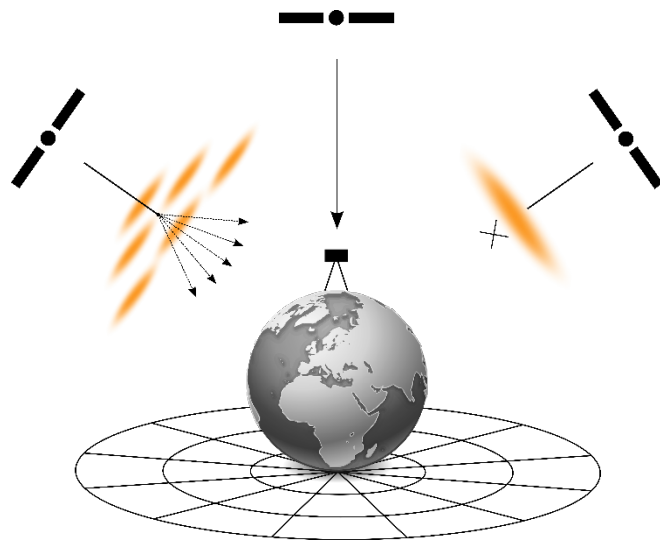
Matthieu Lonchay

PhD Defense

ULiège

Friday 24 May 2019

# Ingestion of Ionospheric Scintillation Skymaps into GNSS Algorithms



Matthieu Lonchay

[M.Lonchay@alumni.uliege.be](mailto:M.Lonchay@alumni.uliege.be)

PhD Defense

ULiège

Friday 24 May 2019